The Thesis Committee for Debojjal Bagchi
certifies that this is the approved version of the following thesis:

Error bounds for stochastic user equilibrium traffic assignment

SUPERVISING COMMITTEE:

Stephen D. Boyles, Supervisor

Zhaomiao Guo

Error bounds for stochastic user equilibrium traffic assignment

by
Debojjal Bagchi

Thesis

Presented to the Faculty of the Graduate School of
The University of Texas at Austin
in Partial Fulfillment
of the Requirements
for the Degree of

Master of Science in Engineering

The University of Texas at Austin
May 2025

Dedication

To my parents

Acknowledgments

My gratitude to everyone whose efforts culminated in this thesis is truly *beyond bounds*. I would first like to express my gratitude to my advisor, Dr. Stephen Boyles, for his guidance over the past two years. This thesis took shape primarily through countless discussions with him. In fact, my interest in stochastic user equilibrium began when I took his course, transportation network analysis, in my first semester at UT Austin. His way of simplifying difficult concepts and offering insights into how someone would come up with a particular theory was highly instrumental in helping me build the foundation of this thesis. He also introduced me to computer algebra systems, which played a significant role in testing several of the proofs in this thesis.

I extend my gratitude to Dr. Zhaomiao Guo for serving as a second reader for the thesis and providing valuable feedback. I am also thankful to Priyararshan Patil, an alumnus of the lab, who had previously worked on finding the numerical evidence that formed the basis for the theory developed in this thesis.

I would like to thank Dr. Raghu Bollapragada for his course on nonlinear programming in the operations research and industrial engineering department, where I learned many of the mathematical techniques I have used in the thesis. I am also thankful to my undergraduate advisor, Dr. Tarun Rambha, who introduced me to the wonderful field of transportation. I got excited about transportation because of his excellent course, which was my first introduction to transportation network analysis.

I would also like to thank other faculty members, especially Dr. Chandra Bhat, Dr. Randy Machemehl, Dr. Tyler Dick, and Dr. Anant Balakrishnan, whose courses were intellectually stimulating and broadened my perspective on transportation.

I convey my gratitude to all members of our research group, Kyle, Jake, Shidong, and Lu, who helped me improve this thesis through several suggestions during our group meetings.

This acknowledgment would be incomplete without mentioning my friends — Sid, Manas, Aranya, Soumili, Sneha, Surya, Sandip, Saurabh, Oihik, and Ainesh. Their encouragement and emotional support have been greatly comforting.

I am deeply grateful to my parents for being the strongest pillars of my motivation. They always kept me encouraged and cheerful, even from thousands of miles away. I am especially thankful to my mother, whose enduring warmth and sense of humor continue to guide me through every challenge, even as she bravely battles metastatic cancer. She is the strongest person I know, and she continues to give me immense strength.

Finally, I would like to thank my girlfriend, Aenakshi, for her constant support and encouragement throughout this period, and for the numerous suggestions that greatly improved the quality of this thesis.

Abstract

Error bounds for stochastic user equilibrium traffic assignment

Debojjal Bagchi, M.S.E
The University of Texas at Austin, 2025

SUPERVISOR: Stephen D. Boyles

In stochastic user equilibrium traffic assignment, we derive bounds on the distance between a given feasible solution and the equilibrium solution. The intent is to provide guidance on termination criteria to reduce runtimes, which is important because the traffic assignment problem is often a subproblem of a more complex bilevel optimization. These mathematical bounds complement existing rules of thumb drawn empirically from numerical case studies.

Our approach is based on Taylor's theorem, applied to the fixed-point formulation of the stochastic user equilibrium assignment, and provides upper bounds on differences in both aggregate metrics (average link travel cost, total system travel time) and disaggregate metrics (link flows, path flows). We demonstrate that the proposed path flow, link flow, and travel cost bounds are tight and cannot be further improved without additional restrictions on the network topology or problem instance.

Results on city-level networks indicate that the bounds on path flows are reasonably tight, with the absolute difference between the derived bound and actual value often in the order of 10^{-1}. We study the tradeoff between the distance from

equilibrium—where the bound becomes applicable—and its tightness. Detailed results guide the choice of a parameter that yields the tightest possible bound for a given distance from equilibrium. Empirical evidence shows that the bound on the distance between any feasible path flow and the equilibrium flow exhibits a near-linear rate of convergence close to equilibrium. This convergence rate is found to be close to 0.9, consistent across all tested networks.

Finally, we demonstrate the practical utility of the derived bounds in a simple network design problem to find optimal link closures. By enumerating the complete feasible set, we show a 36% improvement in computation time on the Sioux Falls network when using the derived bounds, compared to not using them.

Table of Contents

List of Tables

List of Figures

Chapter 1: Introduction

Traffic assignment problems predict the routes travelers are likely to choose based on congestion caused by traffic flow in the network. Algorithms for solving these problems start with a feasible route choice and iteratively improve the solution with the goal of moving closer to an equilibrium solution. Since traffic assignment problems typically involve large-scale nonlinear optimization, reaching an exact equilibrium solution is often computationally expensive. Hence, several stopping criteria are often used to determine if the current solution is reasonably close to the equilibrium solution so that the iterative procedure can be terminated.

While modern solvers can reach near-equilibrium solutions for a single traffic assignment problem within seconds or minutes, many practical applications require solving such problems repeatedly—often tens of thousands of times. This is especially true when the traffic assignment problem has to be solved as a subproblem to a larger optimization framework, such as network design, pricing, Monte Carlo simulation, and other bi-level programs. In such cases early termination becomes particularly important.

Traditional gap functions, such as the difference between the average experienced travel cost and the shortest path travel cost, are used to measure how well the current solution satisfies the equilibrium principle. However, these functions do not directly quantify how close the traffic flows are to equilibrium flows. Researchers have investigated this question numerically, as in the studies by Boyce et al. (2004) and Patil et al. (2021), showing how specific numerical values of a gap function correlate with the convergence of flows and other aggregate metrics (such as total system travel cost and vehicles miles traveled). Patil et al. (2021) show disaggregate metrics such as path flows stabilize within 1% of equilibrium at a relative gap of approximately 10^{-6}. However, more aggregate metrics stabilize earlier — link flows stabilize at a relative gap of around 10^{-5}, and the total system travel cost stabilizes at around 10^{-4}.

In most practical applications, we are primarily interested in aggregate metrics such as travel costs and total system travel cost rather than path flows. Hence, valuable computational resources could be saved by developing a systematic methodology that complements existing numerical results on the convergence behavior of difference metrics at varying gap levels. This would allow the evaluation of a more extensive set of alternatives, which is especially valuable in bi-level optimization programs.

The goal of this thesis is to derive mathematical bounds to complement the extant numerical evidence. In particular, we derive local upper bounds on distance of any feasible path flow solution to the equilibrium solution. Using the result on the bounds on path flows, we also bound the distance of link flows, link cost and total system travel cost of any solution from equilibrium solution.

1.1 Motivation

Consider the following scenario. Suppose n traffic assignment problems have been solved, and consequently, n alternatives have been evaluated as a part of a bi-level optimization problem. While evaluating the $(n+1)^{\text{th}}$ alternative, if it could be determined in early iterations that this alternative would never yield a better equilibrium solution than the n alternatives already evaluated, the $(n+1)^{\text{th}}$ alternative could be terminated quite early, allowing the next alternative to be assessed saving unnecessary computation time.

To develop a theory behind gap functions and convergence in traffic assignment problems, we are interested in estimating the distance between a feasible solution and the equilibrium solution without requiring prior knowledge of the equilibrium itself. For every feasible path flow, we can identify a corresponding target flow that travelers would choose to move toward equilibrium. Note that at equilibrium, the target path flow coincides with the equilibrium path flow. Our goal is to use the distance between a feasible solution and its corresponding target path flow to derive upper bounds on how far the feasible solution is from equilibrium.

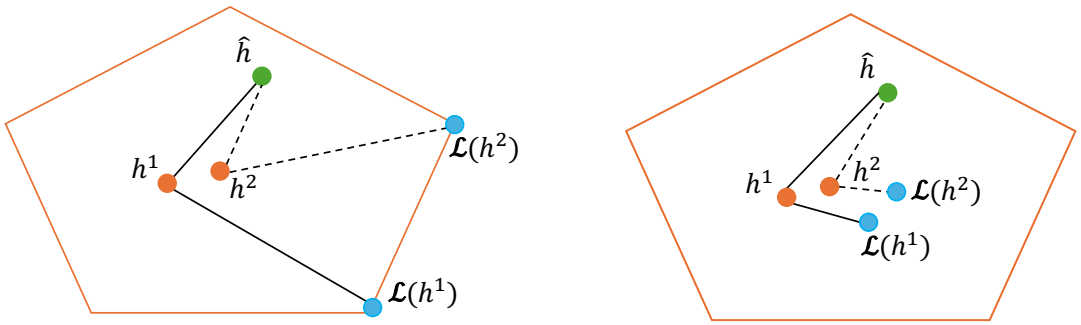

(a) DUE (b) SUE

Figure 1.1: Small perturbation in $\mathbf{h}$ (shown in orange) causes large changes in target flow $\mathcal{L}(\mathbf{h})$ (shown in blue) in DUE, but small changes in SUE. The equilibrium path flow $\hat{\mathbf{h}}$ is shown in green.

To achieve this, we require a model in which the target path flow varies continuously in the current path flows. Hence, we use the stochastic user equilibrium (SUE) model, assuming logit path choice to solve for the traffic assignment problem. Even though the studies by Boyce et al. (2004) and Patil et al. (2021) used deterministic user equilibrium (DUE), a major advantage of SUE for our purposes is that the "target" solution is continuous in the current solution. By contrast, the corresponding map for DUE (the "all-or-nothing assignment") is multivalued whenever paths are tied in cost, and small changes in path costs can cause large shifts in the all-or-nothing assignment. This distinction is explained in Figure 1.1. Figure 1.1a demonstrates how a slight perturbation in path flows, $\mathbf{h}$, can cause a discontinuous jump in the all-or-nothing assignment, $\mathcal{L}(\mathbf{h})$ in DUE. By contrast, Figure 1.1b shows that in SUE, small changes in path flows result in small changes in target flows. The equilibrium solution, $\hat{\mathbf{h}}$, is marked in both figures for reference.

1.2 Objectives

The discussion in Section 1.1 naturally poses the following mathematical question: given a feasible solution to the traffic assignment problem, can we bound its

distance from the equilibrium solution? For instance, if we are only concerned with travel cost, we want to determine an upper bound on how much the travel cost of any particular feasible solution deviates from the equilibrium cost. In this thesis, for any feasible path flow solution close to SUE, we bound its distance from equilibrium, $\|\hat{\mathbf{h}} - \mathbf{h}\|$, in terms of its distance from its target flow, $\|\mathcal{L}(\mathbf{h}) - \mathbf{h}\|$. See Figure 1.1b for reference. The bounds for link flows, link costs, and total system travel cost follow directly.

The research applies to wherever early termination of traffic assignment problems is necessary. Further, from a purely mathematical standpoint, the thesis provides theoretical background on the rule-of-thumb stopping criteria for traffic assignment algorithms. The main objectives of this study are listed below.

1. **Existence of upper bounds.** We present (local) upper bounds on the distance between a feasible path flow solution of the traffic assignment problem and the equilibrium path flows. Using the path flow bounds, we present (local) upper bounds on the distance of aggregate metrics (such as link flows, travel costs, and total system travel cost). The bounds provided are local and only apply close to the equilibrium solution.

2. **Tightness of the proposed bounds.** We show there exists a network where the proposed bounds are tight for any solution. We analyze the tradeoff between the range of applicability and tightness of these upper bounds. Specifically, we provide detailed results on how close to the equilibrium solution these bounds remain applicable and how tight they are.

3. **Convergence of the proposed bounds.** We empirically show that the gap between our proposed path flow bounds and actual distance from equilibrium decreases following a linear convergence rate near equilibrium when method of successive averages is used to solve the stochastic user equilibrium traffic assignment problem.

4. **Computational results on validity and applicability of the proposed bounds.** We present detailed results demonstrating the application of our bounds on the Sioux Falls, Eastern Massachusetts, Berlin Mitte Center, and Anaheim networks. We further demonstrate the practical utility of our proposed bounds using a simple network design problem to find optimal link closures.

1.3 Organization of the thesis

The remainder of the thesis is organized as follows. Chapter 2 reviews existing literature on traffic assignment, SUE, bi-level traffic assignment problems, and mathematical bounds in traffic assignment problems. Chapter 3 presents the logit route choice model and certain well-known mathematical properties of SUE. Chapter 3 also reviews the necessary mathematical background required for the subsequent chapters in the thesis. Chapter 4 presents the main contributions of the thesis—upper bounds on the distance of path flow, link flows, travel cost, and total system travel cost from equilibrium. Chapter 5 follows with the computational results, and 6 concludes the thesis with recommendations and future work.

Chapter 2: Literature Review

2.1 The traffic assignment problem

Traffic assignment problems are route choice models that predict user behavior for a given demand at different origin-destination (OD) pairs under varying congestion levels. These problems can be broadly categorized into static and dynamic models, depending on whether they account for temporal variations in network conditions. A detailed discussion of these models can be found in Boyles et al. (2025).

For long-range planning, static models are generally preferred over dynamic models unless demand is known with high accuracy. This is because it is challenging to predict temporal demand data into the future, and dynamic models are highly sensitive to input data (Boyles and Ruiz Juri, 2019). Static models, on the other hand, are much more reliable, fast, and efficient. Additionally, static traffic assignment enjoys several mathematical properties, including existence, uniqueness, and efficiency of equilibrium, none of which might be true for dynamic traffic assignment (Iryo, 2013).

Traditional traffic assignment models includes link-based methods such as the method of successive averages (MSA), which uses a convex combination of current and target path flows, and Frank-Wolfe's method, which determines the appropriate step size in MSA. Further, there are methods that retain information from all previous iterations of traffic assignment to get an improving direction. A detailed explanation of these algorithms can be found in Boyles et al. (2025). In recent years, there have been a great deal of advancements in solving static traffic assignment models. Some of the state-of-the-art approaches include TAPAS (Bar-Gera, 2010), Algorithm B (Dial, 2006), LUCE (Gentile, 2014), and origin based assignment (Bar-Gera, 2002; Nie, 2012).

2.2 Stochastic traffic assignment

Within static traffic assignment, there are further subdivisions—deterministic and stochastic traffic assignment. Deterministic traffic assignment assumes users have perfect knowledge of travel costs and that travel cost measurements are accurate. In contrast, stochastic traffic assignment relaxes this assumption (Daganzo and Sheffi, 1977), requiring a route choice model based on the distribution of errors between actual and perceived travel costs.

Several route choice models can be used for stochastic traffic assignment. Prashker and Bekhor (2004) extensively review several such route choice models. Specifically, the two main models in this context are the logit model, which assumes independently and identically distributed errors, and the probit model, which accounts for correlations between errors by assuming a multivariate normal distribution.

Despite its ability to model user behavior under imperfect knowledge of travel costs, stochastic traffic assignment with a logit-based route choice model still offers several mathematical properties. Firstly, it is well-known that a stochastic user equilibrium exists and is unique under mild conditions, and can be expressed as the minimum point of a strictly convex function (Boyles et al., 2025; Fisk, 1980). Moreover, the target path flows are continuous in the current path flows. Bar-Gera and Boyce (2006) argue that models with continuous target points have certain advantages, among them that the method of successive averages can actually work quite well if used with a constant step size.

Algorithms developed for solving deterministic traffic assignments can be easily adapted to solve stochastic traffic assignment problems (Boyles et al., 2025). Cantarella and Cascetta (1998) provide a comprehensive summary of several such algorithms and discuss stochastic traffic assignment in detail. The method of successive averages is the most widely used algorithm for solving stochastic traffic assignments. Dial's method (Dial, 1971), later improved by Si et al. (2010), is often employed in the stochastic network loading step in MSA. Further, using a constant

step size (Bar-Gera and Boyce, 2006) in MSA can significantly improve computational efficiency for stochastic traffic assignment. Other algorithms have also been proposed that outperform MSA for specifically logit route choice-based stochastic traffic assignment. For instance, Maher (1998) computes the optimal step length at each iteration, leading to significantly improved convergence. They also explore the use of the Davidon–Fletcher–Powell (DFP) method for determining search direction; however, for large networks, its performance is comparable to that of MSA and worse than the optimal step length approach.

Although various algorithms have improved the efficiency of solving traffic assignment problems, their computational performance remains a concern (Patil et al., 2021), particularly when traffic assignment is used as a subproblem in bilevel optimization and network design. This has led to continued research in speeding up traffic assignment problems as seen in works such as Schneck and Nökel (2020) in DUE and Jiang (2024) in SUE. Jiang (2024) uses a variational inequality formulation for SUE when the choice set is bounded choice to develop efficient algorithms while Schneck and Nökel (2020) use customizable contraction hierarchies for shortest path generation.

2.3 Bi-level traffic assignment

The traffic assignment problem is primarily used in three main applications: evaluating alternatives, highway design, and environmental assessment (Pedersen and Samdahl, 1982; Easa, 1991). When several alternatives have to be evaluated, a bi-level traffic assignment problem is generally necessary. Several examples of situations that would warrant the need for a bi-level traffic assignment are provided below.

Tolling. Pigou (1924) and Knight (1924) were among the first to introduce the concept of a congestion tax, laying the foundation for a vast body of literature on congestion pricing, later popularized by Vickrey (1963, 1969). Tolling or congestion pricing can be used to direct travelers towards system optima (Lindsey* and Verhoef*,

2001; Boyles et al., 2020). De Palma and Lindsey (2011) discuss various strategies for implementing congestion pricing. Beyond guiding users toward the system optimum, tolling can serve several other objectives. For instance, Li et al. (2008) present a Monte Carlo optimization to determine optimal tolls to improve network reliability, Guo and Xu (2016) explore a revenue-maximizing tolling strategy, and Robalino Muñoz (2024) presents equitable tolling approaches. Algorithms to solve congestion pricing problems generally employ a bi-level optimization with the higher level optimizing a particular objective and the lower level solving for traffic assignment.

Network design. The goal of a network design problem is to determine the best investment policy for improving transportation infrastructure. This may involve enhancing certain links to increase capacity (Yang and Bell, 1998a) or, in other cases, closing specific links to prevent Braess's paradox-like scenarios (Korilis et al., 1999; Yang and Bell, 1998b). It could also focus on lane management. For example, Ma et al. (2004) employ a bi-level traffic assignment and genetic algorithm to find optimal lane closures.

OD Matrix estimation. These problems focus on improving the OD matrix obtained from a demand model. OD data from a demand model can sometimes be erroneous and can be combined with flow data from sensors on links to improve the quality of OD data. There are several approaches for OD matrix estimation. Willumsen (1978) and Bera and Rao (2011) review the traditional and state-of-the-art methods used for this purpose respectively. The general idea is to determine a demand matrix such that, when used in a traffic equilibrium model, it produces link flows that match observed sensor data on specific links (Boyles et al., 2025). The problem can be solved heuristically or using a bi-level optimization, both requiring multiple runs of the traffic assignment problem. Yang (1995) reviews several heuristic algorithms for OD matrix estimation.

Network repair. These models deal with finding the optimal strategy to recover a network post-disruption. Rey and Bar-Gera (2020) identify the optimal

sequence in which network recovery tasks should be performed to minimize the total system travel time while Gokalp et al. (2021) identify the sequence in which links should be repaired that minimizes travel cost during the repair horizon. Crocker (2024) presents algorithms to find optimal sequencing of repair on a large number of broken links in both single-crew and multiple-crew settings. All these algorithms require multiple solutions to the traffic assignment problem under different scenarios.

2.4 Convergence and bounds in traffic assignment problems

There have been several studies on the convergence of traffic assignment problems. Mounce and Carey (2015) show that the method of successive averages converges to the equilibrium solution and provide the conditions for a dynamic system (like traffic assignment) to converge to equilibrium when discrete steps are taken. Rose et al. (1988) present the factors determining the magnitude of convergence errors in the Frank-Wolfe algorithm. They argue that it is important to use different stopping criteria based on network configurations and that there is a need for more research in this direction.

Boyce et al. (2004) claim a relative gap of 10^{-4} is required to stabilize link flows. However, the authors point out that the results are only for one network and one demand scenario. Patil et al. (2021) provide a more detailed analysis of the convergence of several aggregate metrics in static traffic assignment. They show more aggregate metrics stabilize at higher relative gap values. For instance, they show total system travel cost and vehicle miles traveled stabilize at around 10^{-4} relative gap, link flows stabilize around 10^{-5} relative gap, while path flows around 10^{-6}. They also claim the results are similar across TAPAS and Algorithm B. The authors pose a major limitation of the study as the results presented are purely empirical and not from a theoretical perspective.

Several studies that aim to establish theoretical bounds on various variables and metrics related to traffic assignment have been presented in the literature. Rough-

garden (2005) presents upper bounds on the price of anarchy, which is defined as the ratio of the total system travel cost at equilibrium to that at the social optimum. Additionally, Roughgarden (2002) shows that the price of anarchy is independent of network topology.

There have been several applications of the price of anarchy in transportation, such as Zhang et al. (2018) and Lazar et al. (2018). Furthermore, studies have explored bounding the price of anarchy in stochastic user equilibrium (Guo et al., 2010). Guo et al. (2010) explain that in stochastic traffic assignment, two types of system optima exist: a deterministic system optimum for the entire network and a stochastic system optimum that accounts for perceived travel times. The study provides bounds for both.

Various strategies have been used in nonlinear optimization to derive error bounds. For instance, Zhou and So (2017) provide techniques to develop error bounds for structured convex optimization problems, where the objective is the sum of a smooth convex function and a closed proper convex function. Such bounds can be used for many constrained minimization problems. Additionally, Facchinei and Pang (2003) present several error bounds in the context of variational inequalities.

2.5 Summary

This chapter reviewed the traffic assignment problem in Section 2.1 and stochastic traffic assignment in Section 2.2. Additionally, we discussed several applications that require multiple runs of a traffic assignment problem in Section 2.3, including congestion pricing, network design, OD matrix estimation, and network repair. Several studies that address each of these problems were reviewed. Most of these solution methods rely on bi-level optimization with traffic assignment at the lower level or heuristics that require multiple runs of the traffic assignment problem.

In Section 2.4, we reviewed studies on the convergence of traffic assignment problems. Works by Boyce et al. (2004) and Patil et al. (2021) propose stopping

criteria for different metrics and observe that different metrics stabilize at different gap measures depending on their level of aggregation. However, both studies are purely empirical and lack a theoretical background.

Furthermore, we discussed how theoretical bounds on specific equilibrium properties have led to widespread applications in transportation research. We further discussed several strategies to derive bounds in non linear convex optimization in Section 2.4. Since stochastic user equilibrium enjoys several mathematical properties as outlined in Chapter 1, a natural research direction is to establish a theoretical background for the empirical convergence measures proposed by Boyce et al. (2004) and Patil et al. (2021), forming the basis of this thesis.

Chapter 3: Background

This chapter provides a detailed description of SUE, outlines its mathematical properties, and introduces the necessary mathematical background for this thesis. Unlike DUE, where all users have perfect knowledge of travel costs, SUE accounts for users' imperfect perception of travel costs. In SUE, users minimize their perceived travel costs between their origin and destination rather than the actual travel costs. Thus, SUE allows for the modeling of perception errors between actual travel costs and the cost a user believes to be actual. An alternative interpretation of users' imperfect perception of travel costs can be thought of as that users may, in fact, have perfect knowledge of travel costs, but the perception error accounts for factors other than travel costs alone. These may include attributes such as road quality or personal preferences not explicitly captured in the travel cost. To formally describe SUE, we first specify how these perception errors are distributed. In this study, we assume a logit choice model to represent these errors, which is further explained in Subsection 3.1. Subsection 3.2 then defines some mathematical properties for SUE under the logit choice model. Finally, Subsection 3.3 presents the necessary mathematical background required for developing the key results of this thesis.

This thesis uses the following notation convention. Vector-valued functions are denoted using calligraphic letters (e.g., $\mathcal{Y}$), and scalar-valued functions are represented by lowercase Greek letters (e.g., γ). Sets are denoted using outlined Roman symbols (e.g., $\mathbb{Y}$). Vectors are represented by bolded lowercase Roman letters (e.g., $\mathbf{y}$), while matrices are denoted by bolded uppercase Roman letters (e.g., $\mathbf{Y}$). Scalars are indicated using Roman letters (e.g., Y or y). The i^{th} component of a vector is written as y_i, while the $(i,j)^{\text{th}}$ component of a matrix is denoted by Y_{ij}. Different instances of a vector are distinguished using superscripts, such as $\mathbf{y}^{(1)}$ and $\mathbf{y}^{(2)}$. The only exception to this convention is π, which is used to denote a path. The notation introduced in this chapter and throughout the thesis is summarized in Table 3.1.

Symbol	Definition
Sets:	
$l \in \mathbb{L}$	Set of links (a) in the network
$\pi \in \mathbb{P}_{OD}$	Set of paths (π) between origin O and destination D
$h_\pi \in \mathbb{H}_{OD}$	Set of path flows (h_π) between origin O and destination D
Vectors:	
$a_i, a_l \in \mathbf{a}$	Vector of link flows (i: index; l: link)
$p_i, p_\pi \in \mathbf{p}$	Vector of probabilities of choosing a path (i: index; π: path)
$c_i, c_\pi \in \mathbf{c}$	Vector of generalized costs of choosing a path (i: index; π: path)
$h_i, h_\pi \in \mathbf{h}$	Vector of path flows (i: index; π: path)
$\hat{h}_i, \hat{h}_\pi \in \hat{\mathbf{h}}$	Vector of SUE path flows (i: index; π: path)
Scalars:	
θ	Logit parameter
d_{OD}	Demand between origin O and destination D
L_γ	Lipschitz constant for function $\gamma(.)$
Matrices:	
$\mathbf{A}, \mathbf{B}$	Generic matrices
$\mathbf{D}$	Link path incidence matrix
Scalar-valued functions:	
$\gamma(.) : \mathbb{R} \to \mathbb{R}$	Generic scalar-valued function
$\tau(a_l) : \mathbb{R} \to \mathbb{R}$	Link cost of link l with flow a_l
Vector-valued functions:	
$\mathcal{F}(.) : \mathbb{R}^m \to \mathbb{R}^n$	Generic vector-valued function
$\mathcal{C}(\mathbf{h}) : \mathbb{R}^n \to \mathbb{R}^n$	Function that outputs cost vector for path flow vector $\mathbf{h}$
$\mathcal{P}(\mathbf{c}) : \mathbb{R}^n \to \mathbb{R}^n$	Function that outputs path-choice probability vector for path cost vector $\mathbf{c}$
$\mathcal{H}(\mathbf{c}) : \mathbb{R}^n \to \mathbb{R}^n$	Function that outputs target path flow vector for cost vector $\mathbf{c}$
$\mathcal{L}(\mathbf{h}) : \mathbb{R}^n \to \mathbb{R}^n$	The logit mapping ($\mathcal{H} \circ \mathcal{C}$) function
$\mathcal{T}(\mathbf{a}) : \mathbb{R}^m \to \mathbb{R}^m$	Function that outputs a vector of link travel times on link with flow $\mathbf{a}$
Matrix-valued functions:	
$\mathcal{C}'(\mathbf{h}) : \mathbb{R}^n \to \mathbb{R}^{n \times n}$	First total derivative of $\mathcal{C}(\mathbf{h})$
$\mathcal{P}'(\mathbf{c}) : \mathbb{R}^n \to \mathbb{R}^{n \times n}$	First total derivative of $\mathcal{P}(\mathbf{c})$
$\mathcal{H}'(\mathbf{c}) : \mathbb{R}^n \to \mathbb{R}^{n \times n}$	First total derivative of $\mathcal{H}(\mathbf{c})$
$\mathcal{L}'(\mathbf{h}) : \mathbb{R}^n \to \mathbb{R}^{n \times n}$	First total derivative of $\mathcal{L}(\mathbf{h})$

Table 3.1: Summary of notation used in this thesis.

3.1 Logit choice model

The logit choice model is a discrete choice model that can be formulated as follows. For each user traveling from origin O to destination D, define $\mathbb{P}_{OD}$ as the set of acyclic paths connecting O to D. Each path $\pi \in \mathbb{P}_{OD}$ is associated with a utility value u_π representing the level of satisfaction the user derives from choosing that

path. The discrete choice model assumes the user chooses the path that maximizes their utility u_π. This utility u_π can be expressed as a sum of two components: the observable part v_π and the unobservable part e_π

$$u_\pi = v_\pi + e_\pi. \tag{3.1}$$

The observed utility, v_π is the portion of the utility visible to the modeler. In our case, we assume it to be the negative generalized travel cost $(-c_\pi)$ for path π. The generalized travel cost is a weighted sum of several factors, such as travel time, tolls, and other monetary costs, all converted into time units using the time value of money. Since a higher cost gives lower utility to a user, we introduce a negative sign.

The unobserved utility, e_π consists of factors that are not explicitly modeled. These might include either user perception errors or factors such as road quality that are not captured by the generalized cost function. Since we do not exactly know e_π, we model it as a random variable to represent user choices probabilistically. In the logit choice model, we assume e_π is independent across paths π and has a Gumbel distribution with zero mean and identical variance. Under this assumption, the probability of choosing a path π is given by

$$p_\pi = \frac{\exp(-\theta c_\pi)}{\sum_{\pi' \in \mathbb{P}_{OD}} \exp(-\theta c_{\pi'})}, \tag{3.2}$$

where θ is a nonnegative parameter chosen to capture the relative importance of the observed and unobserved utility.

3.2 Mathematical properties of SUE

We now introduce relevant notation and explain the mathematical properties of SUE. We denote a path by π and its flow by h_π. The demand between an origin O and a destination D is denoted by d_{OD}. Let $\mathbb{H}_{OD}$ denote the set of feasible path flows between O and D, defined as

$$\mathbb{H}_{OD} = \left\{ h_\pi \;\middle|\; \sum_{\pi \in \mathbb{P}_{OD}} h_\pi = d_{OD}, \quad h_\pi \geq 0 \quad \forall \pi \in \mathbb{P}_{OD} \right\}. \tag{3.3}$$

We denote the set of links in the network by $\mathbb{L}$, where each link is represented by l. The vector of link flows is denoted by $\mathbf{a}$, where a_l is the link flow on link l. The link-path incidence matrix is denoted by $\mathbf{D}$ and is defined as

$$D_{ij} = \begin{cases} 1, & \text{if link } i \text{ is part of path } j, \\ 0, & \text{otherwise.} \end{cases} \tag{3.4}$$

Similarly, the link-path incidence matrix for an origin-destination pair OD, $\mathbf{D}_{OD}$, is defined as

$$(D_{OD})_{ij} = \begin{cases} 1, & \text{if link } i \text{ is part of path } j \text{ in that OD pair,} \\ 0, & \text{otherwise.} \end{cases} \tag{3.5}$$

Let $\mathcal{P}(\mathbf{c})$ denote the vector function given by (3.2), which takes in a vector of path costs $\mathbf{c}$ and outputs the probability of choosing the corresponding paths as a vector $\mathbf{p}$, written as

$$\mathbf{p} = \mathcal{P}(\mathbf{c})\,. \tag{3.6}$$

The *target* flow on a given path h_π is then determined in terms of the path cost vector $\mathbf{c}$ as

$$h_\pi = d_{OD} p_\pi = d_{OD} \frac{\exp(-\theta c_\pi)}{\sum_{\pi'} \exp(-\theta c_{\pi'})}\,, \tag{3.7}$$

where c_π are the components of the cost vector $\mathbf{c}$. We define $\mathcal{H}(\mathbf{c})$ as the vector function corresponding to (3.7), which takes in a vector of path costs $\mathbf{c}$ and outputs the paths the users would choose, represented as

$$\mathbf{h} = \mathcal{H}(\mathbf{c})\,. \tag{3.8}$$

We refer to this as the "target" function because it describes what the path flows *should* be for a given vector of path costs.

Path costs are calculated through network loading. If $\mathbf{a}$ is the vector of link flows, $\mathcal{T}(\mathbf{a})$ represents the vector of link performance functions, and $\mathbf{D}$ is the link-path

incidence matrix, then

$$\mathbf{c} = \mathbf{D}^T \mathcal{T}(\mathbf{a}) = \mathbf{D}^T \mathcal{T}(\mathbf{D}\mathbf{h}) \,. \tag{3.9}$$

We use $\mathcal{C}(\mathbf{h})$ to denote the vector function given by (3.9), which takes a set of path flows $\mathbf{h}$ and outputs the corresponding path costs as $\mathbf{c}$, expressed as

$$\mathbf{c} = \mathcal{C}(\mathbf{h}) \,. \tag{3.10}$$

We denote the vector of equilibrium path flows by $\hat{\mathbf{h}}$. The stochastic user equilibrium can be formulated as the solution to the fixed-point problem: $\hat{\mathbf{h}} = \mathcal{H} \circ \mathcal{C}(\hat{\mathbf{h}})$, for each OD pair. We denote the composite function $\mathcal{H} \circ \mathcal{C}$ as $\mathcal{L}$ and refer to $\mathcal{L}(\mathbf{h})$ as the logit mapping function. Since $\mathcal{L}$ is the composition of continuous and differentiable functions, it is itself continuous and differentiable.

It is well known that stochastic user equilibrium exists and is unique under mild conditions and can be expressed as the minimum point of a strictly convex function (Boyles et al., 2025). The logit mapping ensures that the path flow equilibrium solution is unique as well. While general algorithms exist for solving nonlinear optimization formulations such as the one for SUE, practical road networks introduce tens of thousands of constraints, making direct optimization approaches computationally infeasible. Hence, specialized methods that explore the graph structure are commonly employed. In this thesis, we adopt the MSA algorithm, as outlined in Algorithm 1, to solve for SUE. As demonstrated by Bar-Gera and Boyce (2006), MSA performs considerably well with constant step sizes when target flows are continuous on current flows, as in the case of SUE with logit mapping. We include a comparison of different step size rules in Chapter 5. Further, the main goal of this thesis is to validate our bounds rather than prioritize computational efficiency, making MSA a reasonable choice for solving SUE in our case.

Algorithm 1 Method of successive averages

Initialization: Set the current path flows $\mathbf{h}_{\text{current}}$ and target path flows $\mathbf{h}_{\text{target}}$ to the path flows at free flow conditions.
Set $j = 1$
for *iteration* j **do**
  (a) Choose a step size $s \in [0, 1]$.
  (b) Update the current path flows for each OD pair as

$$\mathbf{h}_{\text{current}} = (1 - s)\mathbf{h}_{\text{current}} + s\mathbf{h}_{\text{target}}.$$

  (c) Compute the updated path costs using the network loading equation (3.9) for each OD pair.
  (d) Update the target path flows using equation (3.8) for each OD pair.
  (e) If $\mathbf{h}_{\text{current}}$ and $\mathbf{h}_{\text{target}}$ are sufficiently close then **terminate**, **else** $j \leftarrow j + 1$.
end

3.3 Mathematical background

We now present the necessary mathematical background for developing the main results of this thesis. We review the total derivative of vector-valued functions, Taylor's theorem, the mean value theorem, key matrix norms, and several vector and matrix inequalities used in our analysis.

Let $\mathcal{F} : \mathbb{R}^n \to \mathbb{R}^m$ be a differentiable function. The Jacobian, or first total derivative, of $\mathcal{F}$ at a point $x \in \mathbb{R}^n$ is defined as the $m \times n$ matrix of first-order partial derivatives:

$$\mathcal{F}'(x) = \begin{bmatrix} \frac{\partial \mathcal{F}_1}{\partial x_1} & \cdots & \frac{\partial \mathcal{F}_1}{\partial x_n} \\ \vdots & \ddots & \vdots \\ \frac{\partial \mathcal{F}_m}{\partial x_1} & \cdots & \frac{\partial \mathcal{F}_m}{\partial x_n} \end{bmatrix}. \tag{3.11}$$

For higher-order derivatives, we consider functions $\mathcal{F} : \mathbb{R}^n \to \mathbb{R}$ that are k-times continuously differentiable ($\mathbb{C}^k$). The Hessian matrix $\mathcal{F}''(x)$ is the second-order derivative given by

$$\mathcal{F}''(x) = \left[\frac{\partial^2 \mathcal{F}}{\partial x_i \partial x_j} \right]_{i,j}. \tag{3.12}$$

For vector-valued functions in several variables, $\mathcal{F} : \mathbb{R}^n \to \mathbb{R}^m$, higher-order derivatives are represented by tensors. For example, the second-order derivative of each component of $\mathcal{F}$ corresponds to a Hessian matrix. Whenever higher-order derivatives of a function of several variables are needed in our analysis, we use Cauchy's estimate (Theorem 1) to estimate their norm. See Gamelin (2003) for a proof for Theorem 1.

Theorem 1 (Cauchy's Estimates)**.** *Suppose f is holomorphic on a neighborhood of the closed ball $\mathbb{B}(z^*, R)$, and suppose that*

$$m := \max\{|f(z)| : |z - z^*| = r\}, \quad (m < \infty). \tag{3.13}$$

Then

$$\left|f^{(n)}(z^*)\right| \leq \frac{n!\, m}{r^n}. \tag{3.14}$$

Throughout this thesis, we assume that all cost functions are holomorphic, allowing us to apply Theorem 1. In practice, most link performance functions and generalized cost functions are holomorphic. In particular, all polynomials are holomorphic. The Bureau of Public Roads (BPR) function (Bureau of Public Roads, 1964), commonly used to calculate travel times, is a polynomial function and is therefore holomorphic. We now state two theorems that we will extensively use throughout the thesis. Theorem 2 is taken from Fusco et al. (2023) and Theorem 3 is taken from Apostol and Ablow (1958).

Theorem 2 (Taylor's theorem with remainder in several variables[1])**.** *Let $\mathcal{F} : \mathbb{R}^n \to \mathbb{R}$ be a function that is $(k+1)$ times continuously differentiable in a neighborhood of $\mathbf{a} \in \mathbb{R}^n$. Then, for $\mathbf{x}$ close to $\mathbf{a}$, $\mathcal{F}(\mathbf{x})$ can be expressed as*

[1]The multi-index notation used in Theorem 2 were primarily taken from Folland (2005) and Lindblad (2011).

$$\mathcal{F}(\mathbf{x}) = \mathcal{F}(\mathbf{a}) + \sum_{i=1}^{n} \mathcal{F}_{x_i}(\mathbf{a})(x_i - a_i) + \frac{1}{2}\sum_{i,j=1}^{n} \mathcal{F}_{x_i x_j}(\mathbf{a})(x_i - a_i)(x_j - a_j)$$
$$+ \cdots + \frac{1}{k!}\sum_{i_1,\ldots,i_k=1}^{n} \mathcal{F}_{x_{i_1}\ldots x_{i_k}}(\mathbf{a})(x_{i_1} - a_{i_1})\cdots(x_{i_k} - a_{i_k}) + \mathcal{R}_k(\mathbf{x} - \mathbf{a}, \mathbf{a}), \tag{3.15}$$

where the remainder term satisfies the bound

$$\|\mathcal{R}_k(\mathbf{x}, \mathbf{a})\| \leq \frac{M}{(k+1)!}\|\mathbf{x} - \mathbf{a}\|^{k+1}, \tag{3.16}$$

provided that

$$\sum_{i_1,\ldots,i_{k+1}=1}^{n} \|\mathcal{F}_{x_{i_1}\ldots x_{i_{k+1}}}(\mathbf{z})\| \leq M, \tag{3.17}$$

for all $\|\mathbf{z} - \mathbf{a}\| \leq \|\mathbf{x} - \mathbf{a}\|$. *The higher-order derivatives are given by*

$$\mathcal{F}_{x_{i_1}\ldots x_{i_k}} = \frac{\partial^k \mathcal{F}}{\partial x_{i_1}\ldots\partial x_{i_k}}. \tag{3.18}$$

Theorem 3 (Mean value theorem for functions of several variables)**.** *If* $\mathbb{S} \subset \mathbb{R}^n$ *is an open set and* $\mathcal{F} : \mathbb{S} \to \mathbb{R}^m$ *is differentiable, then for any two points* $\mathbf{x}, \mathbf{y} \in \mathbb{S}$ *such that the line segment joining* $\mathbf{x}$ *and* $\mathbf{y}$ *is in* $\mathbb{S}$*, there exists a point* $\mathbf{z}^{(\mathbf{i})}$ *along the line segment such that*

$$\mathcal{F}_i(\mathbf{y}) - \mathcal{F}_i(\mathbf{x}) = (\mathcal{F}'(\mathbf{z}^{(\mathbf{i})})(\mathbf{y} - \mathbf{x}))_i. \tag{3.19}$$

for each index $i = 1, \ldots, m$*, where* i *represents the* i*th component of* $\mathcal{F}$.

Observe that the mean value theorem in several variables is the same as applying the mean value theorem in a single variable component-wise. Thus, the point $\mathbf{z}^{(\mathbf{i})}$ is different for each component. Further, the following lemma (Apostol and Ablow, 1958) is a direct consequence of Theorem 3.

Lemma 1. *If* $\mathbb{S}$ *is a convex set, then the line joining* $\mathbf{x}$ *and* $\mathbf{y}$ *is in* $\mathbb{S}$ *for all* $\mathbf{x}, \mathbf{y} \in \mathbb{S}$*, ensuring that the mean value theorem holds globally within* $\mathbb{S}$.

We now define Lipschitz continuity, which provides a bound on the rate of change of a function. The following definition is taken from Courant et al. (1965).

Definition 3.1 (Lipschitz Continuity)**.** A function $\mathcal{F} : \mathbb{R}^n \to \mathbb{R}^m$ is Lipschitz continuous on a set $\mathbb{S} \subseteq \mathbb{R}^n$ if there exists a constant $L_{\mathcal{F}} > 0$ such that

$$|\mathcal{F}(\mathbf{x}) - \mathcal{F}(\mathbf{y})| \leq L_{\mathcal{F}}|\mathbf{x} - \mathbf{y}|, \quad \forall \mathbf{x}, \mathbf{y} \in \mathbb{S}. \tag{3.20}$$

The smallest such constant $L_{\mathcal{F}}$ is called the Lipschitz constant of $\mathcal{F}$.

Next, we define two common norms in linear algebra: the spectral norm and the Frobenius norm.

1. The **spectral norm** (Gentle, 2007) of an $n \times n$ matrix $\mathbf{A}$ is given by

$$\|\mathbf{A}\|_2 = \sup_{\|\mathbf{x}\|=1} \|\mathbf{A}x\|_2, \tag{3.21}$$

   where $\|A\|_2$ is thus the largest singular value of A. For all $x \in \mathbb{R}^n$, the spectral norm satisfies

$$\|\mathbf{A}\mathbf{x}\|_2 \leq \|\mathbf{A}\|_2 \|\mathbf{x}\|_2. \tag{3.22}$$

2. The **Frobenius norm** (Gentle, 2007) of an $n \times n$ matrix $\mathbf{A}$ is defined as

$$\|\mathbf{A}\|_F = \left(\sum_{i,j=1}^{n} |a_{ij}|^2 \right)^{1/2}. \tag{3.23}$$

Furthermore, the spectral norm is bounded by the Frobenius norm as follows:

$$\|\mathbf{A}\|_2 \leq \|\mathbf{A}\|_F \leq \sqrt{n}\|\mathbf{A}\|_2. \tag{3.24}$$

Finally, we present some commonly used matrix and vector inequalities (Theorem 4–6) from Pugh and Pugh (2002).

Theorem 4 (Triangle inequality)**.** *For any vectors* $\mathbf{x}, \mathbf{y}$ *in a normed vector space, the norm satisfies the following triangle inequalities:*

$$\|\mathbf{x}+\mathbf{y}\| \leq \|\mathbf{x}\| + \|\mathbf{y}\|, \text{ and} \tag{3.25}$$

$$\|\mathbf{x}-\mathbf{y}\| \geq \big|\|\mathbf{x}\| - \|\mathbf{y}\|\big|. \tag{3.26}$$

Theorem 5 (Cauchy-Schwarz inequality)**.** *For any two vectors* $\mathbf{x}$ *and* $\mathbf{y}$ *in an inner product space, the inner product satisfies the inequality:*

$$|\langle \mathbf{x}, \mathbf{y} \rangle| \leq \|\mathbf{x}\|\|\mathbf{y}\|. \tag{3.27}$$

Theorem 6 (Sub-multiplicative norm inequality)**.** *Let* $\|\cdot\|$ *be a sub-multiplicative norm on a space of matrices or operators, then for any two matrices* $\mathbf{A}$ *and* $\mathbf{B}$

$$\|\mathbf{AB}\| \leq \|\mathbf{A}\|\|\mathbf{B}\|. \tag{3.28}$$

Chapter 4: Bound formulations

In this chapter, we outline our approach for deriving an upper bound on the distance between any feasible path flow and the equilibrium flow. Upper bounds on link flows and other aggregate metrics follow directly. Our goal is to express the upper bound on the distance between current and equilibrium path flows in terms of current path flows alone. To achieve this, we approximate the logit mapping to the first order around the current path flows and then bound the resulting approximation error.

We begin by analyzing the behavior of the Jacobian over the feasible set of path flows in Section 4.1. We explicitly compute the Jacobian and outline some of its mathematical properties. We also show that the Jacobian and higher derivatives of the logit mapping are bounded under mild assumptions on link costs. Using this knowledge of the derivatives of the logit mapping, we establish bounds on path flows in Section 4.2. The bounds on path flows require two significant assumptions: the cost functions are twice continuously differentiable (i.e., C^2) and the Jacobian of the logit mapping is invertible. To develop bounds on the distance of path flows from equilibrium, we apply the mean value theorem component-wise along the line connecting any feasible path flow solution and the equilibrium solution. The mean value theorem guarantees the existence of a point along this line for each component. We bound the distance from this point to the equilibrium solution using the exact (Lagrange) form of Taylor's theorem in several variables. We then exploit the fixed-point properties of the stochastic user equilibrium (SUE) and employ several linear algebra techniques to bound the distance from any feasible solution to the equilibrium solution. We extend the bound on path flows to aggregate metrics such as link flows, travel costs, and total system travel cost in Section 4.3. The bounds on link flows, travel costs, and total system travel costs follow immediately from the bound on path flows by applying matrix and vector inequalities. Finally, we show that the

bounds on distance of path flows, link flows, and travel cost from equilibrium are tight for a network of parallel links with equal and constant cost functions in Section 4.4. Thus, the proposed bounds cannot be improved without additional information on the network topology or problem instance. However, the proposed bound on the distance of total system travel cost was found to be loose and in fact to never be tight except at equilibrium for the same network.

4.1 Jacobian of the logit mapping

Recall the target path flows at $\mathbf{h}$ are given by the logit mapping, $\mathcal{L}(\mathbf{h})$. We need to calculate the partial derivatives $\frac{\partial \mathcal{L}_i}{\partial h_j}$ to fill out the Jacobian. This is slightly tricky because if we change just h_j and no other path flow, we are also changing the total demand. To be careful, we will re-specify the mapping $\mathcal{L}$ in a more general way that allows d_{OD} to vary and derive its Jacobian. The i^{th} component of the Jacobian can be computed as

$$\mathcal{L}(\mathbf{h})_i = \sum_j h_j \cdot \frac{\exp(-\theta c_i)}{\sum_j \exp(-\theta c_j)} = \sum_j h_j \cdot p_i. \tag{4.1}$$

We then re-specify $\mathcal{H}$ as

$$\mathcal{H}(\mathbf{c}) = \mathcal{H}(\mathbf{h}, \mathbf{p}). \tag{4.2}$$

Applying the chain rule, the Jacobian of $\mathcal{L}(\mathbf{h}) = \mathcal{H}(\mathbf{h}, \mathcal{P}(\mathcal{C}(\mathbf{h})))$ with respect to $\mathbf{h}$ is

$$\mathcal{L}'(\mathbf{h}) = \mathcal{H}'(\mathbf{h}) + \mathcal{H}'(\mathbf{p}) \cdot \mathcal{P}'(\mathbf{c}) \cdot \mathcal{C}'(\mathbf{h}). \tag{4.3}$$

Going through the calculus, we find each matrix as follows.

1. In $\mathcal{H}'(\mathbf{h})$, we treat $\mathbf{p}$ as constant and find that $\frac{\partial \mathcal{L}_i}{\partial h_j} = p_i$. The Jacobian $\mathcal{H}'(\mathbf{h})$ is, therefore, a matrix where each row consists of the same value p_i.

2. We calculate $\mathcal{H}'(\mathbf{p})$ to be a diagonal matrix with elements $\sum_j h_j$ (that is, the current demand d_{OD}).

3. The elements of $\mathcal{P}'(\mathbf{c})$ are the sensitivities of the logit model with respect to path costs. As computed in Koppelman and Bhat (2006), they are given by

$$(\mathcal{P}'(\mathbf{c}))_{ij} = \begin{cases} -\theta \cdot p_i \cdot (1 - p_i) & \text{if } i = j, \\ \theta \cdot p_i \cdot p_j & \text{if } i \neq j. \end{cases} \tag{4.4}$$

4. Finally, we have the Jacobian of the path costs with respect to path flows $\mathcal{C}'(\mathbf{h})$; the element in the i-th row and j-th column of $\mathcal{C}'(\mathbf{h})$ is the derivative of path i's cost with respect to flow on path j, which is the sum of the link cost derivatives on the links belonging to both paths

$$\frac{\partial \mathcal{C}_i}{\partial h_j} = \sum_{l \in \pi_i \cap \pi_j} \tau'(a_l), \tag{4.5}$$

where $\tau(a_l)$ is the link cost of link l with flow a_l.

Given the description of the Jacobian, the following lemma immediately follows.

Lemma 2. *The product of the Jacobian $\mathcal{H}'(\mathbf{h})$ and the difference of any two feasible path flows in the same OD pair is zero.*

Proof. The product of the Jacobian $\mathcal{H}'(\mathbf{h})$ with any vector $\mathbf{h}^{(1)}$ can be calculated as follows. The i-th component of $\mathcal{H}'(\mathbf{h}).\mathbf{h}^{(1)}$ is

$$(\mathcal{H}'(\mathbf{h}).\mathbf{h}^{(1)})_i = \sum_j p_i h_j^{(1)} = p_i \sum_j h_j^{(1)} = p_i.d_{OD}\,. \tag{4.6}$$

Therefore, for any two *feasible* path flows $\mathbf{h}^{(1)}$ and $\mathbf{h}^{(2)}$ in the same OD pair, $\mathcal{H}'(h) \cdot (\mathbf{h}^{(1)} - \mathbf{h}^{(2)}) = d_{OD}\mathbf{p} - d_{OD}\mathbf{p} = \mathbf{0}$. □

We define

$$\mathcal{K}(\mathbf{h}) := \mathcal{H}'(\mathbf{p}) \cdot \mathcal{P}'(\mathbf{c}) \cdot \mathcal{C}'(\mathbf{h}). \tag{4.7}$$

Since the path costs $\mathbf{c}$ depend on the path flows $\mathbf{h}$, and the probabilities $\mathbf{p}$ depend on the path costs $\mathbf{c}$, we can express $\mathcal{K}$ solely in terms of the path flows $\mathbf{h}$. This definition of $\mathcal{K}$ later simplifies our calculations, since

$$\mathcal{L}'(\mathbf{h})(\mathbf{h}^{(1)} - \mathbf{h}^{(2)}) = \mathcal{H}'(\mathbf{h})(\mathbf{h}^{(1)} - \mathbf{h}^{(2)}) + \mathcal{H}'(\mathbf{p})\mathcal{P}'(\mathbf{c})\mathcal{C}'(\mathbf{h})(\mathbf{h}^{(1)} - \mathbf{h}^{(2)}) \tag{4.8}$$

$$= \mathcal{H}'(\mathbf{h})(\mathbf{h}^{(1)} - \mathbf{h}^{(2)}) + \mathcal{K}(\mathbf{h})(\mathbf{h}^{(1)} - \mathbf{h}^{(2)}) \tag{4.9}$$

$$= \mathcal{K}(\mathbf{h})(\mathbf{h}^{(1)} - \mathbf{h}^{(2)}). \tag{4.10}$$

Since our primary goal is to obtain a first-order expansion of the logit mapping $\mathcal{L}$, it is essential that the Jacobian of $\mathcal{L}$ is bounded. In fact, it suffices to show that $\mathcal{K}$ is bounded. We present the following theorem to show that $\mathcal{K}$ is indeed bounded in the set of feasible path flows under reasonable assumptions on link costs.

Theorem 7. *Suppose the cost functions are in C^1. Then, the difference $\left(\frac{\partial \mathcal{C}_k}{\partial h_j} - \frac{\partial \mathcal{C}_i}{\partial h_j}\right)$ is bounded. Further, the function $\mathcal{K}(\mathbf{h})$ is bounded; i.e., there exist constants $\underline{m_0}$ and $\overline{m_0}$ such that*

(a) $\underline{m_0} \leq \left(\frac{\partial \mathcal{C}_k}{\partial h_j} - \frac{\partial \mathcal{C}_i}{\partial h_j}\right) \leq \overline{m_0}$, *and*

(b) $d_{OD}\theta\underline{m_0} \leq \mathcal{K}_{ij}(\mathbf{h}) \leq d_{OD}\theta\overline{m_0}$.

Proof. We begin by analyzing component-wise. We look at the i^{th} component of $\mathcal{K}(\mathbf{h})$. The matrix $\mathcal{H}'(\mathbf{p})$ is diagonal with d_{OD} as its diagonal elements. The i^{th} row of $\mathcal{H}'(\mathbf{p})$ contains d_{OD} in the i^{th} position and zeros elsewhere. When $\mathcal{H}'(\mathbf{p})$ is multiplied by $\mathcal{P}'(\mathbf{c})$, this will pick up the i^{th} column of $\mathcal{P}'(\mathbf{c})$. With some simple algebraic simplifications, we can show that

$$(\mathcal{K}(\mathbf{h}))_i = (\mathcal{H}'(\mathbf{p}) \cdot \mathcal{P}'(\mathbf{c}) \cdot \mathcal{C}'(\mathbf{h}))_i \tag{4.11}$$

$$= d_{OD}\theta \begin{bmatrix} p_i p_1 & \cdots & -p_i(1-p_i) & \cdots & p_1 p_n \end{bmatrix} \cdot \begin{bmatrix} (\mathcal{C}'(\mathbf{h}))_1 \\ (\mathcal{C}'(\mathbf{h}))_2 \\ \vdots \\ (\mathcal{C}'(\mathbf{h}))_n \end{bmatrix} \tag{4.12}$$

$$= d_{OD}\theta \sum_{k=1,k\neq i}^{n} (p_i p_k (\mathcal{C}'(\mathbf{h}))_k) - p_i(1-p_i)\left((\mathcal{C}'(\mathbf{h}))_i\right) \tag{4.13}$$

$$= d_{OD}\theta p_i \sum_{k=1,k\neq i}^{n} (p_k (\mathcal{C}'(\mathbf{h}))_k) - p_i(1-p_i)\left((\mathcal{C}'(\mathbf{h}))_i\right) \tag{4.14}$$

$$= d_{OD}\theta p_i \sum_{k=1,k\neq i}^{n} (p_k (\mathcal{C}'(\mathbf{h}))_k) - p_i \left(\sum_{k=1,k\neq i}^{n} p_k \right) \left((\mathcal{C}'(\mathbf{h}))_i\right) \tag{4.15}$$

$$= d_{OD}\theta p_i \sum_{k=1,k\neq i}^{n} (p_k (\mathcal{C}'(\mathbf{h}))_k - (\mathcal{C}'(\mathbf{h}))_i) \tag{4.16}$$

$$= d_{OD}\theta p_i \sum_{k=1,k\neq i}^{n} (p_k (\mathcal{C}'(\mathbf{h}))_k - (\mathcal{C}'(\mathbf{h}))_i) \tag{4.17}$$

The cost functions are assumed to be C^1. Hence, the derivatives must be continuous. The feasible set of path flows is closed and bounded, hence compact. Continuous functions on compact sets are bounded. The difference of bounded functions is also bounded. Hence there exists $\underline{m_0}$ and $\overline{m_0}$, such that $\underline{m_0} \leq \left(\frac{\partial \mathcal{C}_k}{\partial z_j} - \frac{\partial \mathcal{C}_i}{\partial z_j} \right) \leq \overline{m_0}$ for all i, j, k. Further, the probabilities (p_i) are always less than one. This completes the proof. □

As a consequence of Theorem 7, we can readily bound the higher-order derivatives of $\mathcal{K}$, which are necessary for estimating the error in the first-order approximation of the logit mapping. Since these higher-order derivatives are tensors, we apply Cauchy's estimates (Theorem 5) to bound their norm rather than computing them explicitly. Lemma 3 computed these upper bounds.

Lemma 3. *Suppose the cost functions are twice continuously differentiable, then the first derivative of $\mathcal{K}$ is bounded. i.e., there exists m_1 such that*

$$||\mathcal{K}'(\mathbf{h})|| \leq m_1. \tag{4.18}$$

Proof. The proof follows directly from Theorem 7 and from the fact that the domain for feasible path flows is compact. Since the cost functions are assumed to be twice continuously differentiable, we know there exists some m_1 such that

$$\|\mathcal{K}^{(n)}(\mathbf{h})\| \leq m_1. \tag{4.19}$$

If we assume the cost functions are holomorphic, then m_1 can be computed using Cauchy's estimates (Theorem 1). We clarify the meaning of $\|\mathcal{K}^{(1)}(\mathbf{h})\|$ in this context. $\mathcal{K}(\mathbf{h})$ is a product of three $n \times n$ Jacobian matrices as defined in Equation (4.7). The derivatives of $\mathcal{K}(\mathbf{h})$ consist of multiple Hessian matrices, one corresponding to each component row of $\mathcal{K}(\mathbf{h})$. The notation $\|\mathcal{K}'(\mathbf{h})\|$ refers to the maximum of all such bounds on each of these Hessian matrices.

4.2 Bounds on path flows

This section presents the first key result of this thesis. Theorem 8 establishes an upper bound on the distance between current path flows and equilibrium path flows. To derive this bound, we use our understanding of the Jacobian and its higher-order derivatives, along with the results from the previous section. The derivation in this section follows some concepts from Bar-Gera and Boyce (2006) and the fixed point property of SUE described in Section 3.2.

Theorem 8 (Local Bound)**.** *Suppose the cost functions are C^2. Then, for any $r_{OD} \in [0, 1)$, there exists constants m_1, m_2, and e_h such that for all feasible path flows $\mathbf{h}_{OD}$ in an origin-destination (OD) pair satisfying $\|\mathbf{h}_{OD} - \hat{\mathbf{h}}_{OD}\| \leq e_{hr}^{OD}$, the norm of the difference between the current and equilibrium path flows is bounded by a factor*

depending only on the current path flows, i.e., $\|\hat{\mathbf{h}}_{OD} - \mathbf{h}_{OD}\| \leq M_{hr}^{OD} \|\mathcal{L}(\mathbf{h}_{OD}) - \mathbf{h}_{OD}\|$, *where*

(i) $M_{hr}^{OD} = \|(I - \mathcal{K}(\mathbf{h}_{OD}))^{-1}\| \frac{1}{1-r_{OD}}$,

(ii) $e_{hr}^{OD} = \frac{r_{OD}}{\|(I-\mathcal{K}(\mathbf{h}_{OD}))^{-1}\|(m_1+m_2)}$.

Proof. For brevity, we will omit the subscript and superscript OD in the rest of the proof when not necessary. Given any two feasible path flows $\mathbf{h}, \hat{\mathbf{h}} \in \mathbb{H}_{OD} \subset \mathbb{R}^n$, where $\mathbb{H}_{OD}$ is convex, the line segment connecting $\mathbf{h}$ and $\hat{\mathbf{h}}$ is contained within $\mathbb{H}_{OD}$. Since $\mathcal{L}$ is differentiable on $\mathbb{H}_{OD}$ (by Theorem 7), applying the mean value theorem (Theorem 3) component-wise, there exists a point $\mathbf{h}^{(i)}$ along the line segment joining $\mathbf{h}$ and $\hat{\mathbf{h}}$ such that

$$\{\mathcal{L}_i(\hat{\mathbf{h}}) - \mathcal{L}_i(\mathbf{h})\} = (\{\mathcal{L}'(\mathbf{h}^{(i)})(\hat{\mathbf{h}} - \mathbf{h})\})_i. \tag{4.20}$$

Since the SUE path flows are a fixed point to the logit mapping, it follows that

$$\mathcal{L}(\hat{\mathbf{h}}) = \hat{\mathbf{h}}. \tag{4.21}$$

Using Equation (4.20) and substituting for $\mathcal{L}(\hat{\mathbf{h}})$ using (4.21) it follows

$$\{\mathcal{L}_i(\hat{\mathbf{h}}) - \mathcal{L}_i(\mathbf{h})\} = \{\mathcal{L}'(\mathbf{h}^{(i)})(\hat{\mathbf{h}} - \mathbf{h})\}_i \text{ and} \tag{4.22}$$

$$\{\hat{\mathbf{h}}_i - \mathcal{L}_i(\mathbf{h})\} = \{\mathcal{K}(\mathbf{h}^{(i)})(\hat{\mathbf{h}} - \mathbf{h})\}_i. \tag{4.23}$$

Equation (4.23) follows from Lemma 2 and Equation (4.10). Observe that Equation (4.23) is a scalar equation, as we are considering only the i^{th} component of the vectors. This equation depends on the current ($\mathbf{h}$) and equilibrium ($\hat{\mathbf{h}}$) path flows, except for $\mathbf{h}^{(i)}$, which lies along the line segment connecting $\mathbf{h}$ and $\hat{\mathbf{h}}$. Therefore, if we can bound the difference between $\mathbf{h}^{(i)}$ and $\mathbf{h}$, we obtain the desired bound. We define $\mathcal{W}_i(\mathbf{h}^{(i)}) = \mathcal{K}(\mathbf{h}^{(i)})(\hat{\mathbf{h}} - \mathbf{h})_i$ for each component i. We then approximate $\mathcal{W}_i(\mathbf{h}^{(i)})$ around $\mathbf{h}$ using a first-order Taylor expansion as

$$\mathcal{W}_i(\mathbf{h}^{(i)}) - \mathcal{W}_i(\mathbf{h}) = \mathcal{W}_i'(\mathbf{h})(\mathbf{h}^{(i)} - \mathbf{h}) + R_2(\mathbf{h}^{(i)}), \tag{4.24}$$

where $R_2(\mathbf{h}^{(i)})$ is a second-order term that grows with $\|\mathbf{h}^{(i)}-\mathbf{h}\|^2$. Equation (4.24) represents the exact form of the first-order Taylor expansion (Theorem 2) applied to $\mathcal{W}_i$. Taking the norm on both sides of Equation (4.24) and applying the sub-multiplicative norm inequality (Theorem 6) along with the triangle inequality (Theorem 4), we obtain

$$|\mathcal{W}_i(\mathbf{h}^{(i)}) - \mathcal{W}_i(\mathbf{h})| \leq \|\mathcal{W}_i'(\mathbf{h})(\mathbf{h}^{(i)} - \mathbf{h})\| + \|R_2(\mathbf{h}^{(i)})\|. \tag{4.25}$$

With some linear algebra, we obtain

$$\begin{aligned}
|\mathcal{W}_i(\mathbf{h}^{(i)}) - \mathcal{W}_i(\mathbf{h})| &\leq \|\mathcal{W}_i'(\mathbf{h})\|\|\mathbf{h}^{(i)} - \mathbf{h}\| + m_2\|\mathbf{h}^{(i)} - \mathbf{h}\|^2 && (4.26)\\
&\leq \|\mathcal{W}_i'(\mathbf{h})\|\|\hat{\mathbf{h}} - \mathbf{h}\| + m_2\|\hat{\mathbf{h}} - \mathbf{h}\|^2 && (4.27)\\
&\leq \|\mathcal{K}'(\mathbf{h}^{(i)})\|\|(\hat{\mathbf{h}} - \mathbf{h})\|^2 + m_2\|\hat{\mathbf{h}} - \mathbf{h}\|^2 && (4.28)\\
&\leq m_1\|\hat{\mathbf{h}} - \mathbf{h}\|^2 + m_2\|\hat{\mathbf{h}} - \mathbf{h}\|^2. && (4.29)
\end{aligned}$$

Inequality (4.26) follows from the Cauchy–Schwarz inequality (Theorem 5) and the bound on the second-order Taylor remainder (Theorem 2). Inequality (4.27) uses the fact that $\mathbf{h}^{(i)}$ lies between $\mathbf{h}$ and $\hat{\mathbf{h}}$. Inequality (4.28) follows from the definition of $\mathcal{W}$ and another application of the Cauchy–Schwarz inequality. Finally, Inequality (4.29) follows from Lemma 3. Thus, as a consequence of Equation (4.23) and Inequality (4.29), we obtain the following:

- $\{\hat{\mathbf{h}}_i - \mathcal{L}_i(\mathbf{h})\} = \{\mathcal{K}(\mathbf{h}^{(i)})(\hat{\mathbf{h}} - \mathbf{h})\}_i$ (Equation (4.23)) and,
- $|\mathcal{K}(\mathbf{h}^{(i)})(\hat{\mathbf{h}} - \mathbf{h})_i - \mathcal{K}(\mathbf{h})(\hat{\mathbf{h}} - \mathbf{h})_i| \leq (m_1 + m_2)\|\hat{\mathbf{h}} - \mathbf{h}\|^2$ (Equation (4.29)).

Combining the two equations yields

$$|\hat{\mathbf{h}}_i - \mathcal{L}_i(\mathbf{h}) - \{\mathcal{K}(\mathbf{h})(\hat{\mathbf{h}} - \mathbf{h})\}_i| \leq (m_1 + m_2)\|\hat{\mathbf{h}} - \mathbf{h}\|^2. \tag{4.30}$$

Since Equation (4.30) applies component-wise, we can combine all the components to get the vector equation

$$\|\hat{\mathbf{h}} - \mathcal{L}(\mathbf{h}) - \mathcal{K}(\mathbf{h})(\hat{\mathbf{h}} - \mathbf{h})\| \leq (m_1 + m_2)\|\hat{\mathbf{h}} - \mathbf{h}\|^2. \tag{4.31}$$

$$\text{or, } \|(\mathcal{L}(\mathbf{h}) - \mathbf{h}) - (\mathbf{I} - \mathcal{K}(\mathbf{h}))(\hat{\mathbf{h}} - \mathbf{h})\| \leq (m_1 + m_2)\|\hat{\mathbf{h}} - \mathbf{h}\|^2, \tag{4.32}$$

where $\mathbf{I}$ denotes the identity matrix. Equation (4.32) follows directly from Equation (4.31) via elementary algebraic manipulations. Next, we multiply both sides by $\|(\mathbf{I} - \mathcal{K}(\mathbf{h}))^{-1}\|$ and apply the sub-multiplicative norm inequality (Theorem 6), yielding

$$\begin{aligned}
&\|(\mathbf{I} - \mathcal{K}(\mathbf{h}))^{-1}(\mathcal{L}(\mathbf{h}) - \mathbf{h}) - (\hat{\mathbf{h}} - \mathbf{h})\| \\
&\leq \|(\mathbf{I} - \mathcal{K}(\mathbf{h}))^{-1}\| \cdot \|(\mathcal{L}(\mathbf{h}) - \mathbf{h}) - (\mathbf{I} - \mathcal{K}(\mathbf{h}))(\hat{\mathbf{h}} - \mathbf{h})\| \\
&\leq (m_1 + m_2)\|(\mathbf{I} - \mathcal{K}(\mathbf{h}))^{-1}\| \cdot \|\hat{\mathbf{h}} - \mathbf{h}\|^2. \qquad (4.33)
\end{aligned}$$

Applying the triangle inequality (Theorem 4) and the Cauchy-Schwarz inequality (Theorem 5) to (4.33), we obtain

$$\begin{aligned}
&|\|(\mathbf{I} - \mathcal{K}(\mathbf{h}))^{-1}\|\|(\mathcal{L}(\mathbf{h}) - \mathbf{h})\| - \|(\hat{\mathbf{h}} - \mathbf{h})\|| \\
&\leq (m_1 + m_2)\|(\mathbf{I} - \mathcal{K}(\mathbf{h}))^{-1}\| \cdot \|\hat{\mathbf{h}} - \mathbf{h}\|^2. \qquad (4.34)
\end{aligned}$$

Finally, by eliminating the absolute difference, we get

$$\begin{aligned}
&\|(\hat{\mathbf{h}} - \mathbf{h})\| - \|(\mathbf{I} - \mathcal{K}(\mathbf{h}))^{-1}\|\|(\mathcal{L}(\mathbf{h}) - \mathbf{h})\| \\
&\leq (m_1 + m_2)\|(\mathbf{I} - \mathcal{K}(\mathbf{h}))^{-1}\| \cdot \|\hat{\mathbf{h}} - \mathbf{h}\|^2. \qquad (4.35)
\end{aligned}$$

Observe that Inequality (4.35) involves only current and equilibrium path flows. If $\mathbf{h}$ is sufficiently close to $\hat{\mathbf{h}}$, we can assume $\|\hat{\mathbf{h}} - \mathbf{h}\|^2 \approx 0$, thereby providing the required bound. We now formalize this argument mathematically.

For any given $r \geq 0$, we define e_{hr} as

$$e_{hr} = \frac{r}{\|(\mathbf{I} - \mathcal{K}(\mathbf{h}))^{-1}\|(m_1 + m_2)}. \qquad (4.36)$$

This allows us to linearize the quadratic $\|\hat{\mathbf{h}} - \mathbf{h}\|^2$ term in Inequality (4.35). For any feasible path flow, $\mathbf{h}$ satisfying $\|\hat{\mathbf{h}} - \mathbf{h}\| \leq e_{hr}$ we have

$$\|(\mathbf{I} - \mathcal{K}(\mathbf{h}))^{-1}\|(m_1 + m_2)\|\hat{\mathbf{h}} - \mathbf{h}\|^2 \leq r\|\hat{\mathbf{h}} - \mathbf{h}\|. \qquad (4.37)$$

Substituting Inequality (4.37) into Inequality (4.35), we derive

$$\|(\hat{\mathbf{h}} - \mathbf{h})\| - r\|\hat{\mathbf{h}} - \mathbf{h}\| \leq \|\mathbf{I} - \mathcal{K}(\mathbf{h}))^{-1}(\mathcal{L}(\mathbf{h}) - \mathbf{h})\|. \qquad (4.38)$$

Rearranging Inequality (4.38) and applying the sub-multiplicative norm inequality, we derive the result

$$\|(\hat{\mathbf{h}} - \mathbf{h})\| \leq \frac{\|(\mathbf{I} - \mathcal{K}(\mathbf{h}))^{-1}\|}{1 - r} \|(\mathcal{L}(\mathbf{h}) - \mathbf{h})\|. \tag{4.39}$$

This concludes the proof. □

Before proceeding to provide bounds on aggregate metrics, we develop an intuition for the values of r. The bound in (4.39) applies for any value of $r \in [0, 1)$ as long as $\|\hat{\mathbf{h}} - \mathbf{h}\| \leq e_{hr}$. The parameter r controls how far from equilibrium the bounds begin to hold. Note that from the definition of e_{hr} in (4.36) that for larger values of r, the bound applies from a greater distance from equilibrium but tends to be weaker. Conversely, for smaller r, the bound holds closer to equilibrium and becomes tighter. At equilibrium, the bound is tight with the parameter r set to zero.

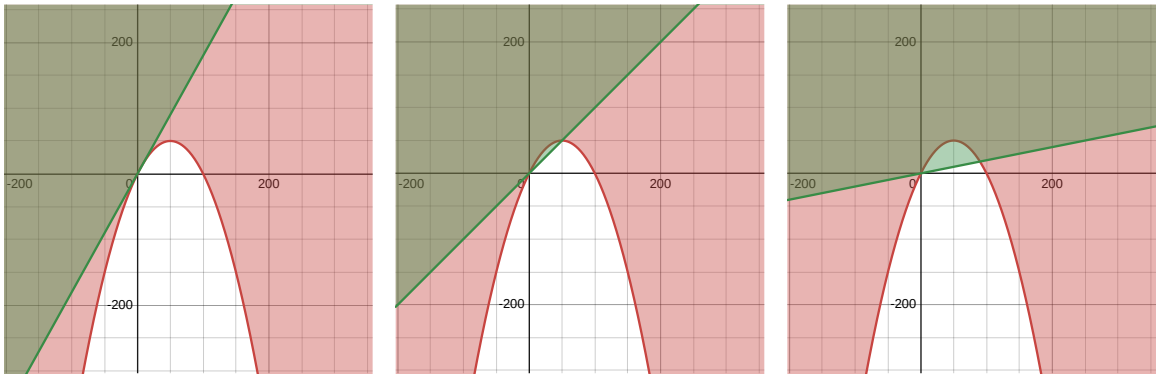

(a) $r = 0.1$ (b) $r = 0.5$ (c) $r = 0.9$

Figure 4.1: Linearizing technique: Red shading shows $x \leq 0.5y + 0.01x^2$ and the green shading shows $x \leq \frac{0.5}{1-r}y$.

A simpler illustration of the intuition behind the linearizing technique used in Equations (4.36)–(4.39) is provided in Figure 4.1. Figure 4.1 shows the quadratic inequality $x \leq 0.5y + 0.01x^2$ being approximated by the linear inequality $x \leq \frac{0.5}{1-r}y$. The three subfigures demonstrate that as x approaches zero, the linear approximation improves but holds for a smaller range of values. For instance, when $r = 0.1$, the linear

approximation (shown in green) closely matches the quadratic inequality (shown in red), but it remains valid only up to $x = 18$. Beyond $x = 18$, the linear approximation no longer holds, as indicated by the red shaded region not covered by the green region. On the other hand, when $r = 0.9$, the bound holds more loosely (as seen in the green region not overlapping with the red region), but it remains valid up to $x = 90$.

In the example shown in Figure 4.1, x corresponds to $\|\hat{\mathbf{h}} - \mathbf{h}\|$, and y corresponds to $\|\mathcal{L}(\mathbf{h}) - \mathbf{h}\|$. Since these are positive quantities, we are only interested in the first quadrant of these plots. Consequently, as r approaches one, the linear approximation holds true for the entire region. However, in this case, $\frac{1}{1-r}$ becomes extremely large, making the bound too loose to be useful. Therefore, choosing an appropriate value of r is crucial. Further analysis on the parameter r is provided in Chapter 5.

4.3 Bounds on aggregate metrics

The bounds on link flow and travel cost follow directly from Theorem 8. To simplify notation, we denote $\|\hat{\mathbf{h}}_{OD} - \mathbf{h}_{OD}\|$ as $\|\hat{\mathbf{h}} - \mathbf{h}\|_{OD}$. The following lemma presents the results on bounds on aggregate metrics.

Lemma 4 (Bound on link flows and travel time)**.** *Suppose the conditions of Theorem 8 hold, with*

$$\|\hat{\mathbf{h}} - \mathbf{h}\|_{OD} \leq M_{hr}^{OD} \|\mathcal{L}(\mathbf{h}) - \mathbf{h}\|_{OD}, \tag{4.40}$$

and that the travel cost functions have bounded derivatives, are Lipschitz continuous, and there are no link interactions. Then the following holds:

(a) ***Bound on link flows:***

$$\|\mathbf{a} - \hat{\mathbf{a}}\| \leq \sum_{OD} \|\mathbf{D}_{OD}\| M_{hr}^{OD} \|\mathcal{L}(\mathbf{h}) - \mathbf{h}\|_{OD}. \tag{4.41}$$

(b) ***Bound on travel cost:***

$$\|\mathcal{T}(\mathbf{a}) - \mathcal{T}(\hat{\mathbf{a}})\| \leq L_{\mathcal{T}} \sum_{OD} \|\mathbf{D}_{OD}\| M_{hr}^{OD} \|\mathcal{L}(\mathbf{h}) - \mathbf{h}\|_{OD}, \tag{4.42}$$

where $L_{\mathcal{T}}$ is the Lipschitz constant for the function $\mathcal{T}$.

Proof. We begin by expressing the norm of the difference between $\mathbf{a}$ and $\hat{\mathbf{a}}$ in terms of path flows using the link path incidence matrix $\mathbf{D}$

$$\|\mathbf{a} - \hat{\mathbf{a}}\| = \left\| \sum_{OD} \mathbf{D}_{OD}\mathbf{h} - \sum_{OD} \mathbf{D}_{OD}\hat{\mathbf{h}} \right\| \tag{4.43}$$

$$= \left\| \sum_{OD} \mathbf{D}_{OD}(\mathbf{h} - \hat{\mathbf{h}}) \right\|. \tag{4.44}$$

Applying the triangle inequality and sub-multiplicative norm inequality, we obtain

$$\left\| \sum_{OD} \mathbf{D}_{OD}(\mathbf{h} - \hat{\mathbf{h}}) \right\| \leq \sum_{OD} \left\| \mathbf{D}_{OD}(\mathbf{h} - \hat{\mathbf{h}}) \right\| \tag{4.45}$$

$$\leq \sum_{OD} \|\mathbf{D}_{OD}\| \cdot \|\mathbf{h} - \hat{\mathbf{h}}\|_{OD}. \tag{4.46}$$

Finally, we invoke Theorem 8 to get the result

$$\sum_{OD} \|\mathbf{D}_{OD}\| \cdot \|\mathbf{h} - \hat{\mathbf{h}}\|_{OD} \leq \sum_{OD} \|\mathbf{D}_{OD}\| \cdot M_{hr}^{OD} \|\mathcal{L}(\mathbf{h}) - \mathbf{h}\|_{OD}.$$

□

To bound the travel costs, we employ a similar set of steps with the additional assumption that the travel cost function, $\mathcal{T}$, is Lipschitz continuous with Lipschitz constant $L_{\mathcal{T}}$. This implies

$$\|\mathcal{T}(\mathbf{a}) - \mathcal{T}(\hat{\mathbf{a}})\| = ||\mathcal{T}(\sum_{OD} \mathbf{D}_{OD})\mathbf{h} - \mathcal{T}(\sum_{OD} \mathbf{D}_{OD}\hat{\mathbf{h}})|| \tag{4.47}$$

$$\leq L_{\mathcal{T}} \sum_{OD} \|\mathbf{D}_{OD}\| . M_{hr}^{OD} \|\mathcal{L}(\mathbf{h}) - \mathbf{h}\|_{OD}. \tag{4.48}$$

This completes the proof. □

If we assume that the travel cost functions follow BPR (Highway Capacity Manual, 2000) functions and link flow cannot exceed its capacity, we can compute the Lipschitz constant $L_{\mathcal{T}}$ directly. Since BPR functions have bounded derivatives, we can use the fact that an everywhere differentiable function $\gamma : \mathbb{R} \to \mathbb{R}$ is Lipschitz continuous with Lipschitz constant given by $\sup |\gamma'(x)|$. Suppose the cost of link l is given by

$$\tau_l(a) = u_l \cdot \left(1 + f\left(\frac{a}{c_l}\right)^g\right) + hT_l, \tag{4.49}$$

where u_l is the free-flow travel time of link l, c_l is its capacity, f and g are parameters of the BPR function, h is the time value of money, and T_l is the toll on that link. To compute the Lipschitz constant, we take the derivative with respect to a as $\tau_l'(a) = u_l \cdot f \cdot g \cdot c_l^{-g} \cdot a^{g-1}$. Since the Lipschitz constant is defined as $L_{\mathcal{T}} = \sup_{a \geq 0} |\tau_l'(a)|$, we obtain,

$$L_{\mathcal{T}} = \sup_{a \geq 0} \left| u_l \cdot f \cdot g \cdot c_l^{-g} \cdot a^{g-1} \right|. \tag{4.50}$$

For $g > 1$, the supremum occurs at the maximum feasible flow, which is capacity ($a = c_l$), giving

$$L_{\mathcal{T}} = \max_l \left(\frac{f g u_l}{c_l}\right) = f g \max_l \left(\frac{u_l}{c_l}\right). \tag{4.51}$$

Lemma 5 (Bound on total system travel time)**.** *Suppose the conditions of Theorem 8 holds, i.e.,*

$$\|\hat{\mathbf{h}} - \mathbf{h}\|_{OD} \leq M_{hr}^{OD} \|\mathcal{L}(\mathbf{h}) - \mathbf{h}\|_{OD}, \tag{4.52}$$

and that the travel cost functions have bounded derivatives, are Lipschitz continuous, and there are no link interactions. Then the following upper bound exists on total system travel time:

$$\mathcal{T}(\hat{\mathbf{a}}) \cdot \hat{\mathbf{a}} \leq (\|\mathbf{a}\| + M_L)(\|\mathcal{T}(\mathbf{a})\| + L_{\mathcal{T}} M_L). \tag{4.53}$$

Here,

$$M_L = \sum_{OD} \|\mathbf{D}_{OD}\| \cdot M_{hr}^{OD} \|\mathcal{L}(\mathbf{h}) - \mathbf{h}\|_{OD}. \tag{4.54}$$

Proof. We know from Lemma 4

$$\|\mathbf{a} - \hat{\mathbf{a}}\| \leq M_L, \implies \|\hat{\mathbf{a}}\| \leq \|\mathbf{a}\| + M_L \tag{4.55}$$

$$\text{and} \quad \|\mathcal{T}(\mathbf{a}) - \mathcal{T}(\hat{\mathbf{a}})\| \leq L_{\mathcal{T}} M_L \implies \|\mathcal{T}(\hat{\mathbf{a}})\| \leq \|\mathcal{T}(\mathbf{a})\| + L_{\mathcal{T}} M_L. \tag{4.56}$$

Combining inequalities (4.55) and (4.56) and using the Cauchy-Schwarz inequality and the fact that total system travel cost is always nonnegative, we get

$$\mathcal{T}(\hat{\mathbf{a}}) \cdot \hat{\mathbf{a}} \leq \|\hat{\mathbf{a}}\| \|\mathcal{T}(\hat{\mathbf{a}})\| \leq (\|\mathbf{a}\| + M_L)(\|\mathcal{T}(\mathbf{a})\| + L_{\mathcal{T}} M_L). \tag{4.57}$$

This completes the proof. □

4.4 Tightness of the proposed bounds

We now demonstrate that the derived bounds on path flows (in Theorem 8), link flows in (Lemma 4a), and travel cost (in Lemma 4b) are always tight for a network of parallel links for any globally feasible solution. Further, the bound on total system travel cost (in Lemma 5) is never tight for this network unless at equilibrium.

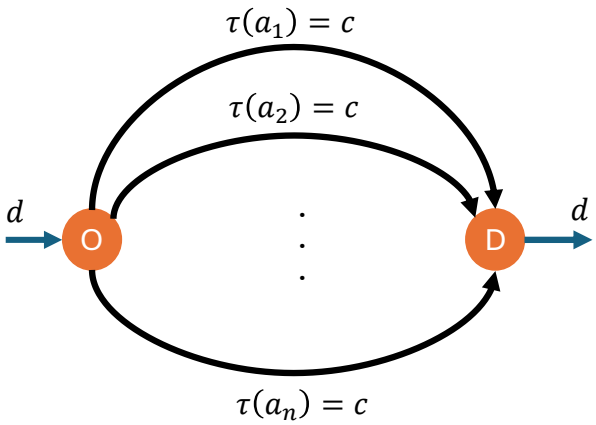

Figure 4.2: Network of parallel links.

Consider a network with one OD pair and n parallel links, all having equal and constant cost functions $\tau(a_l) = c$ as shown in Figure 4.2. Then $\mathcal{C}'(\mathbf{h}) = 0$, by

Equation (4.5) and consequently $\mathcal{K}(\mathbf{h})$ is also a zero matrix by Equation (4.7). Take $r = 0$ for the tightest bound. Hence, M_{hr} in Theorem 8 is one. For any path flow $\mathbf{h}$, observe $\mathcal{L}(\mathbf{h}) = \hat{\mathbf{h}} = [d/n, \ldots d/n]$. Hence $\|\hat{\mathbf{h}} - \mathbf{h}\| = M_{hr}\|\mathcal{L}(\mathbf{h}) - \mathbf{h}\|$. Therefore, the bound in Theorem 8 is tight for any path feasible flow in this network.

Observe that the link path incidence matrix is an identity for the same network. Hence, $\|\mathbf{D}\| = 1$ in Lemma 4. The link flows and path flows are the same for this network. Thus, $\|\mathbf{a} - \hat{\mathbf{a}}\| = \sum_{OD} \|\mathbf{D}_{OD}\| M_{hr}^{OD} \|\mathcal{L}(\mathbf{h}) - \mathbf{h}\|_{OD} = \|\mathcal{L}(\mathbf{h}) - \mathbf{h}\|$, showing that the bounds in Lemma 4(a) hold with equality for this network for any feasible link flow. Constant functions have a Lipschitz constant of zero, and hence $\|\mathcal{T}(\mathbf{a}) - \mathcal{T}(\hat{\mathbf{a}})\| \leq L_{\mathcal{T}} \sum_{OD} \|\mathbf{D}_{OD}\| M_{hr}^{OD} \|\mathcal{L}(\mathbf{h}) - \mathbf{h}\|_{OD} = 0$, showing that the bound in 4(b) holds with equality for any feasible solution.

For any path flows $\mathbf{h}$, the total system travel cost is the same as demand times the constant travel time, i.e., $\hat{\mathbf{a}}.\mathcal{T}(\hat{\mathbf{a}}) = \mathbf{a}.\mathcal{T}(\mathbf{a}) = cd$. We showed M_L in Lemma 5 is $\|\mathcal{L}(\mathbf{h}) - \mathbf{h}\|$. Hence, the bound on total system travel cost is never tight for this network, as the upper bound in Lemma 5 always exceeds cd, except when $M_l = 0$, which happens only at equilibrium.

Chapter 5: Results

The bounds derived in Chapter 4 were tested on real-world transportation networks. All experiments were run in Python 3.12.5 and on an Apple MacBook Air with an M2 chip, an 8-core CPU, an 8-core GPU, and 16 GB of unified memory. We tested the derived bounds on the Sioux Falls, Berlin-Mitte-Center, Anaheim, and Eastern Massachusetts networks. The data required for these networks, including network structure and demand, is publicly available at Transportation Networks for Research Core Team (2025). Table 5.1 provides a summary of these networks.

Network	**OD pairs**	**Links**	**Nodes**	**Total demand**
Sioux Falls	24^2	76	24	360600.0
Berlin-Mitte-Center (BMC)	36^2	871	398	11481.9
Eastern-Massachusetts (EMA)	74^2	258	74	65576.4
Anaheim	38^2	914	416	10469.4

Table 5.1: Networks used in the study.

The method of successive averages (Algorithm 1) was used to solve for SUE. As discussed in Chapter 3, the continuous nature of the logit mapping allows MSA to be used with a constant step size. In fact, with appropriate adjustments, using a constant step size can lead to much faster convergence to SUE compared to using a reciprocal iteration number as a step size. The step size selection strategy used in our implementation of MSA is outlined in Algorithm 2. A FIFO queue is used to track the last three gap values. For the first ten iterations, we reduce the step size as the reciprocal of the iteration number. Thereafter, a constant step size is used until the gap function reduces by more than 1% in the last three iterations. In case it doesn't, the step size is reset to the reciprocal of the iteration number.

Algorithm 2 Step size selection

Input: i (iteration number), $\mathbf{g}$ (FIFO list of last 3 gap values)
Output: s (step size for iteration i)

```
if i ≤ 10 then
    s ← 1/i
else
    if |g2 − g0| / g0 < 0.01 then
        s ← 1/i
```

The gap function was chosen to be the difference between current and target path flows, i.e., $\|\mathbf{h} - \mathcal{L}(\mathbf{h})\|$. The proposed step size selection rule results in significantly faster convergence compared to the traditional approach of setting the step size as the reciprocal of the iteration number. A comparison is provided in Table 5.2. In Table 5.2, "Rule 1" refers to step size set as the reciprocal of iteration count, whereas "Rule 2" refers to step size determined by Algorithm 2. A maximum of ten minutes was provided to the MSA algorithm to converge with either step size selection rule. If MSA failed to converge to the specified gap within ten minutes, it is indicated by a "−" in Table 5.2. As shown in Table 5.2, "Rule 2" demonstrates remarkably faster convergence than "Rule 1." Due to the computational performance produced by constant step sizes, all our tests were performed using Algorithm 2.

Gap	**Sioux Falls**		**BMC**		**EMA**		**Anaheim**	
$\|\mathbf{h} - \mathcal{L}(\mathbf{h})\|$	Rule 1	Rule 2	Rule 1	Rule 2	Rule 1	Rule 2	Rule 1	Rule 2
10000	11.1	4.7	13.5	13.5	55.8	54.4	132.4	107.7
1000	104.5	8.5	134.7	115.6	574.1	163.4	-	284.2
100	-	12.4	-	264.5	-	272.3	-	452.9
10	-	16.2	-	413.9	-	376.0	-	
1	-	20	-	562.7	-	490.6	-	-

Table 5.2: Computation time (in seconds) to reach desired gap level using Rule 1 and Rule 2 for step size selection across different networks. Rule 1 sets step size as the reciprocal of iteration, while Rule 2 sets step size as per Algorithm 2. "-" means gap value was not achieved in 10 min timespan.

In all our experiments, the equilibrium solution was assumed to be the first path flow solution satisfying $\|\mathbf{h}-\mathcal{L}(\mathbf{h})\| \leq 1$. The path set for each OD pair was taken as the ten shortest paths within that OD pair, and the logit parameter (θ) was fixed at 0.5. The initial solution in all experiments was assumed to be path flow given by logit network loading at free flow. Table 5.3 provides the time to calculate the bounds. Table 5.3 mentions the time for each iteration of MSA with and without calculating the bounds. The time to calculate with bounds includes the time to calculate path flow bounds on all OD pairs, the bounds on link flows, travel cost, and the total system travel cost for each iteration.

Network	**Time without bounds**	**Time with bounds**	**Time to calculate bounds**
Sioux Falls	0.18	0.25	0.07
BMC	6.71	7.08	0.37
EMA	4.95	5.24	0.29
Anaheim	7.56	8.08	0.52

Table 5.3: Computation times (in seconds) for different networks with and without bounds. (Times in an average of first five iterations.)

The bounds on path flows derived in Theorem 8, and the aggregate metrics presented in Lemma 4 and Lemma 5 were verified until the gap value satisfied $\|\mathbf{h} - \mathcal{L}(\mathbf{h})\| \leq 10$. The results are presented in the subsequent sections. Section 5.1 presents results on path flow bounds, while Section 5.2 evaluates the bounds on aggregate metrics such as link flows, travel time, and total system travel time. Finally, Section 5.3 demonstrates the benefits of using these bounds in a network design problem. To foster collaborative research, the source code for all experiments is made available on GitHub[1].

[1] github.com/debojjalb/SUE_Bounds

5.1 Results on path flow bounds

We present the results on the tightness and accuracy of the bound derived on path flows in Theorem 8. Recall that Theorem 8 provided an upper bound on the distance between the current path flow solution and the equilibrium solution based on just the current path flow solution. However, this is only a local bound, meaning it is valid only "close" to equilibrium.

The parameter $0 \leq r < 1$ in Theorem 8 determines how close to the equilibrium the bound would remain applicable. For smaller values of r, the bound is much tighter but applies only close to equilibrium, while when r approaches one, the bound remains valid much farther from equilibrium but is significantly looser. We define a metric called *bound gap* for each OD pair to quantify the tightness of the derived bounds. The bound gap for a OD pair at a iteration i of MSA is defined as

$$\mathrm{BG}^{OD}_{i^{\text{th}}\text{ iteration}} = \Big(|\|\mathbf{h} - \hat{\mathbf{h}}\|_{OD} - M^{OD}_{hr} \|\mathcal{L}(\mathbf{h}) - \mathbf{h}\|_{OD}| \Big)_{i^{\text{th}}\text{ iteration}}. \tag{5.1}$$

We then define the bound gap across all the OD pair as

$$\mathrm{BG}_{i^{\text{th}}\text{ iteration}} = \sum_{OD} \mathrm{BG}^{OD}_{i^{\text{th}}\text{ iteration}}. \tag{5.2}$$

When the bound gap is computed for the iteration corresponding to a gap value of one, we denote it as BG without a subscript. To identify the value of r that balances tightness and applicability of the derived bound on path flows, we test the bound across a range of r values. The results are summarized in Table 5.4.

	Sioux Falls			BMC			EMA			Anaheim		
r	It.	Gap	BG	It.	Gap	BG	It.	Gap	BG	It.	Gap	BG
0.1	106	2.4	0.68	54	19.3	0.70	10	11431	0.56	33	1475.6	0.55
0.2	105	2.7	0.77	35	141.5	0.78	10	11431	0.63	15	9868.1	0.62
0.3	48	1082.9	0.88	24	447.5	0.89	10	11431	0.72	9	18610	0.71
0.4	45	1649.4	1.0	17	929.3	1.0	10	11431	0.84	3	56269.9	0.82
0.5	43	2036.1	1.2	13	1408.2	1.3	10	11431	1.0	3	56269.9	0.99
0.6	42	2262.5	1.5	10	1920.6	1.6	10	11431	1.3	3	56269.9	1.2
0.7	24	13722.1	2.1	8	2387.9	2.1	10	11431	1.7	2	86713.2	1.7
0.8	18	26260.1	3.1	3	6259	3.1	10	11431	2.5	2	86713.2	2.5
0.9	17	29295.3	6.2	3	6259	6.3	10	11431	5.1	2	86713.2	4.9
Ref.	115	1		83	1		99	1		103	1	

Table 5.4: MSA iteration (It.) and gap ($\|\mathbf{h}-\mathcal{L}(\mathbf{h})\|$) values when the path flow bound first holds in all OD pairs for different networks at various r values. The reference row indicates the number of iterations required by MSA to reach a gap level of one (equilibrium solution). The BG column presents the bound gap if the MSA was run until a gap value of one for a particular value of r. A lower bound gap means the bound is tighter.

Table 5.4 presents the iteration count and the corresponding threshold gap value ($|\mathbf{h} - \mathcal{L}(\mathbf{h})|$) at which the bounds first hold for *all* OD pairs in the network. It also reports the bound gap (BG) for several values of r, assuming the MSA is run until the gap reduces to one. A lower BG indicates a tighter bound. It is important to note that we do not claim the bounds continue to hold for all subsequent iterations after iteration i, even if they hold at i. While empirical evidence suggests that the bounds typically hold beyond the iteration presented in Table 5.4 for most OD pairs in the tested networks, there are cases where they do not hold for certain OD pairs until a significantly smaller gap is reached.

It is observed that as the values of r become larger, the bound holds from quite far from equilibrium and is loose, while for smaller values of r, the bound is much tighter and holds close to equilibrium. The effect of the parameter r is particularly evident in the Sioux Falls network. Hence, we show the bound for two values of r in the Sioux Falls network in Figure 5.1 to illustrate the effect of r on the tightness and

applicability of the bound.

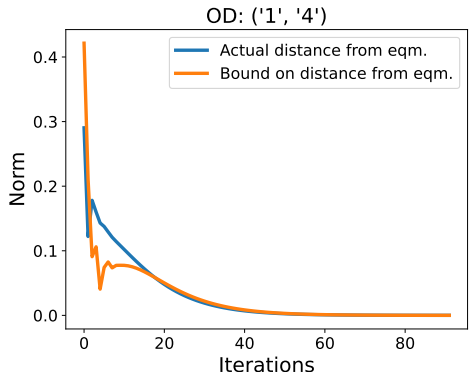

(a) $r = 0.2$, linear norm scale.

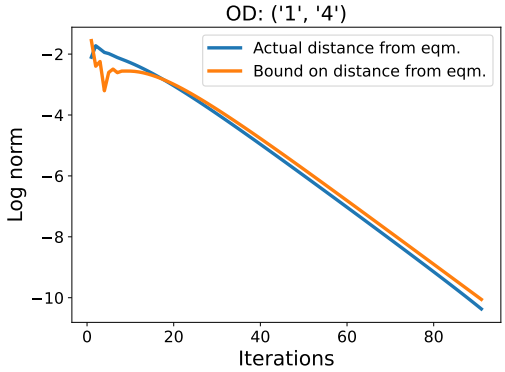

(b) $r = 0.2$, log norm scale.

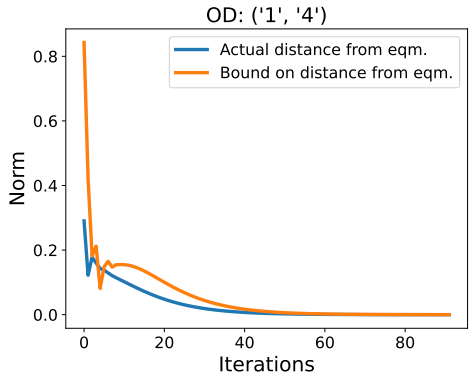

(c) $r = 0.6$, linear norm scale.

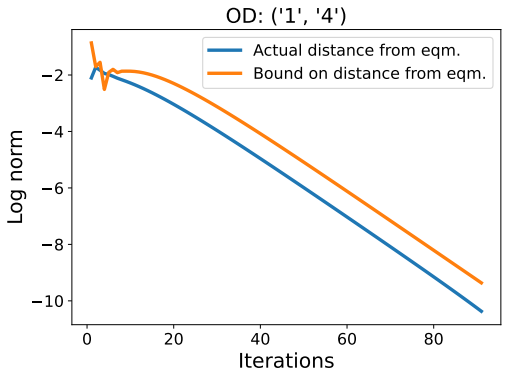

(d) $r = 0.6$, log norm scale.

Figure 5.1: Sioux Falls bound on path flows with different r values. The orange line represents the bound $M_{hr}^{OD}\|\mathcal{L}(\mathbf{h}) - \mathbf{h}\|_{OD}$, while the blue line depicts the actual distance from equilibrium $\|\hat{\mathbf{h}} - \mathbf{h}\|_{OD}$. The x-axis denotes the number of MSA iterations, and the y-axis represents the norm value in Figures 5.1 and 5.3 and the log norm value in 5.2 and 5.4.

For the remainder of our experiments, we chose an r value of 0.4 as it strikes the right balance between tightness and applicability of the bound. The bounds derived in this study are particularly useful in practical scenarios where multiple traffic assignment runs are required under varying conditions. We recommend selecting an appropriate r value by first solving the traffic assignment to SUE once for the specific

network under study. Once the value of r is chosen and the corresponding threshold gap is known, reasonably accurate estimates of flow-based metrics at equilibrium can be obtained by solving the traffic assignment only until the threshold gap is reached, significantly reducing computational time.

We next present detailed results on path flow bounds and convergence for each network. Figures 5.2, 5.4, 5.6, and 5.8 show the actual distance from equilibrium, $\|\mathbf{h}-\hat{\mathbf{h}}\|_{OD}$, alongside our derived bound, $M_{hr}^{OD}\|\mathcal{L}(\mathbf{h})-\mathbf{h}\|_{OD}$, for 16 randomly selected OD pairs at every iteration of MSA in the Sioux Falls, BMC, EMA, and Anaheim networks, respectively. The blue line shows the actual distance for equilibrium, and the orange line shows the upper bound. We emphasize that obtaining every point on the blue line requires knowledge of the equilibrium path flow $\hat{\mathbf{h}}$, whereas each point on the orange line can be computed just from the current path flow $\mathbf{h}$.

To further assess the effectiveness of the bound near equilibrium, we provide the semilog plots corresponding to Figures 5.2, 5.4, 5.6, and 5.8 in Figures 5.3, 5.5, 5.7, and 5.9. These plots show the log of the actual distance from equilibrium and the bound over iterations. The slope of both lines in the semilog plot is similar, indicating a linear rate of convergence.

Sioux Falls

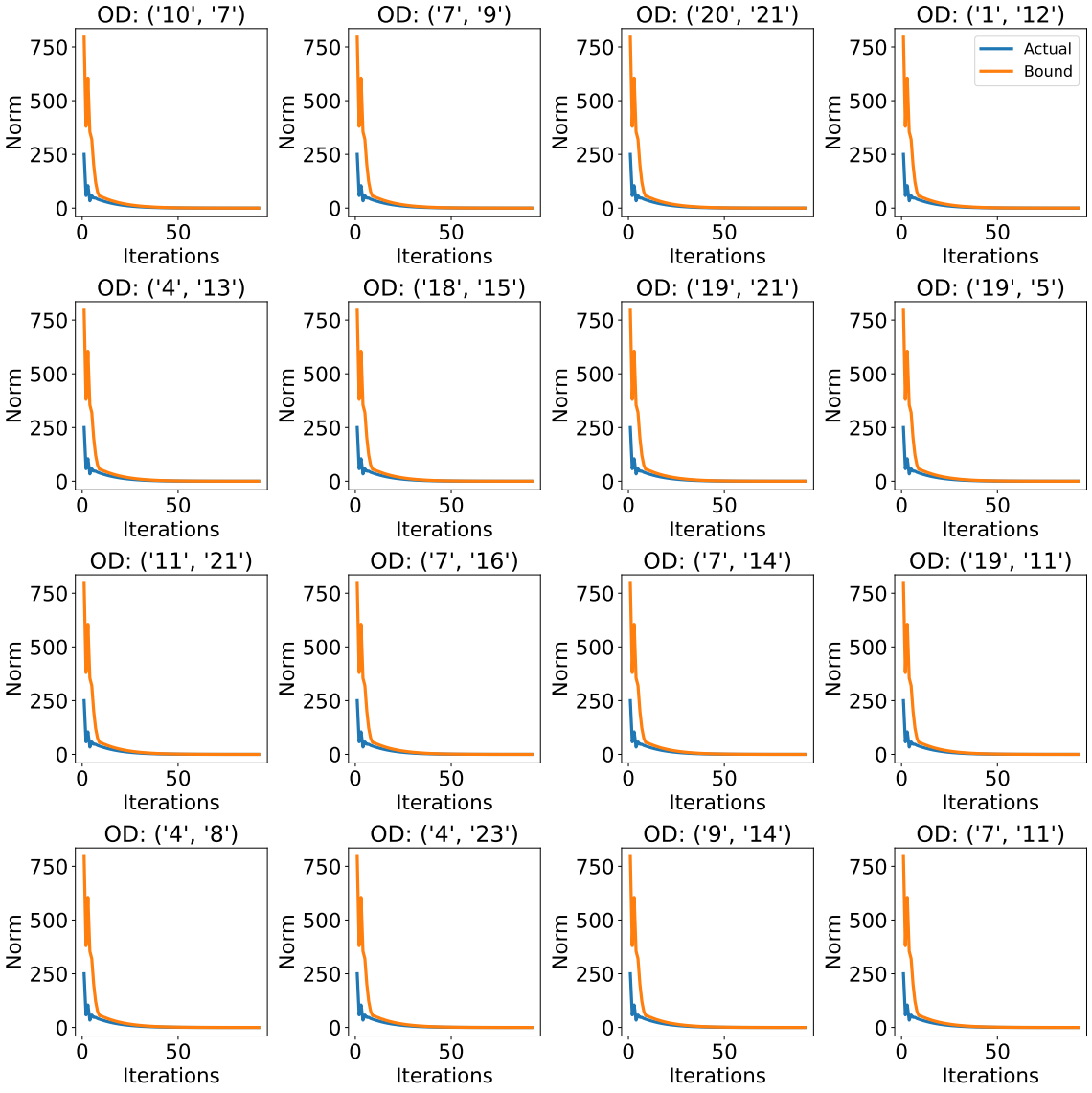

Figure 5.2: Sioux Falls - Path bound for 16 random OD pairs. The orange line represents the bound $M_{hr}^{OD}\|\mathcal{L}(\mathbf{h})-\mathbf{h}\|_{OD}$, while the blue line depicts the actual distance from equilibrium $\|\hat{\mathbf{h}}-\mathbf{h}\|_{OD}$. The x-axis denotes the number of MSA iterations, and the y-axis represents the norm value.

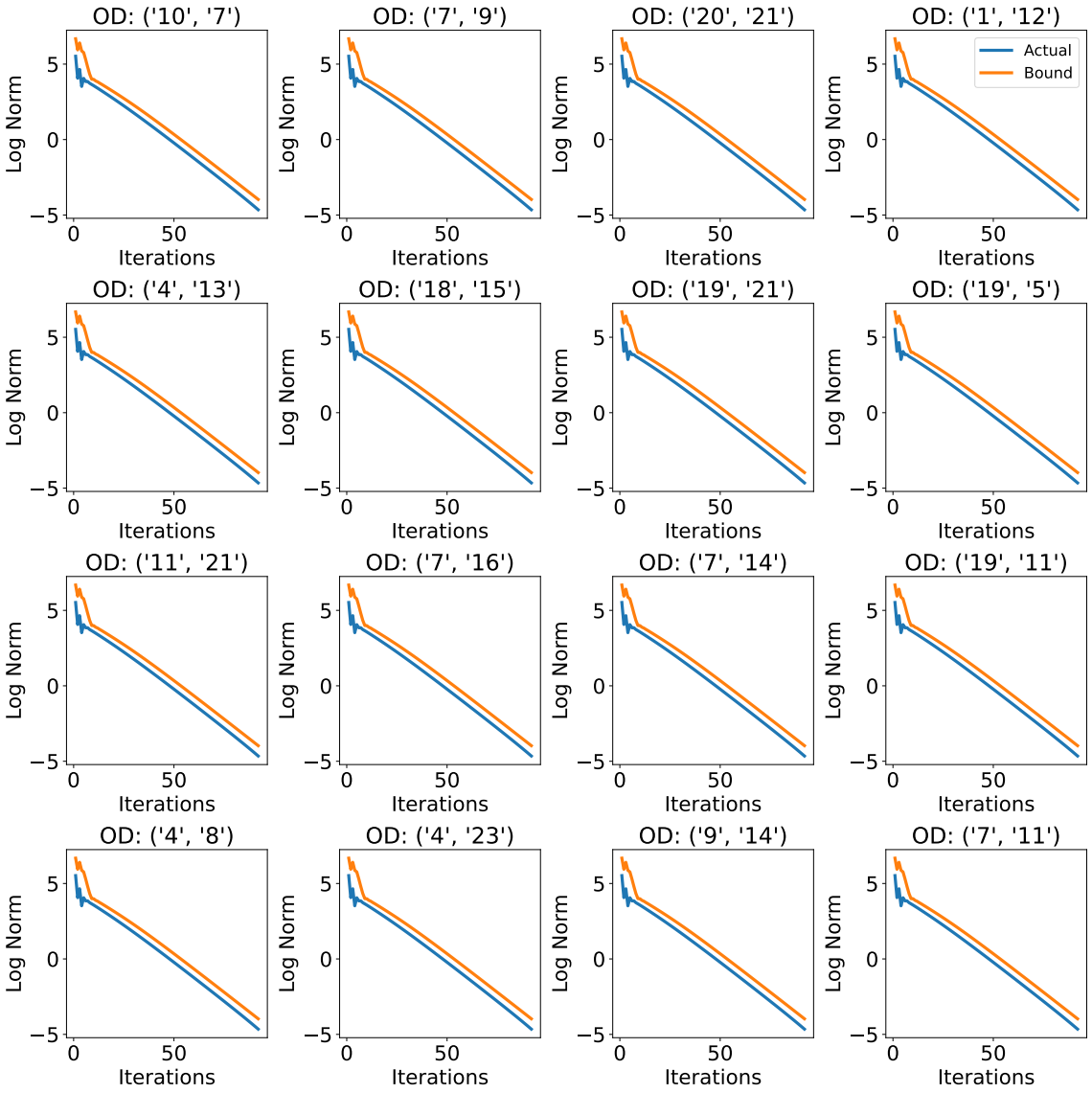

Figure 5.3: Sioux Falls - Semilog plot of all iterations for path bound for 16 random OD pairs. The orange line represents the bound $M_{hr}^{OD}\|\mathcal{L}(\mathbf{h}) - \mathbf{h}\|_{OD}$, while the blue line depicts the actual distance from equilibrium $\|\hat{\mathbf{h}} - \mathbf{h}\|_{OD}$. The x-axis denotes the number of MSA iterations, and the y-axis represents the log of the norm value.

Berlin-Mitte-Center

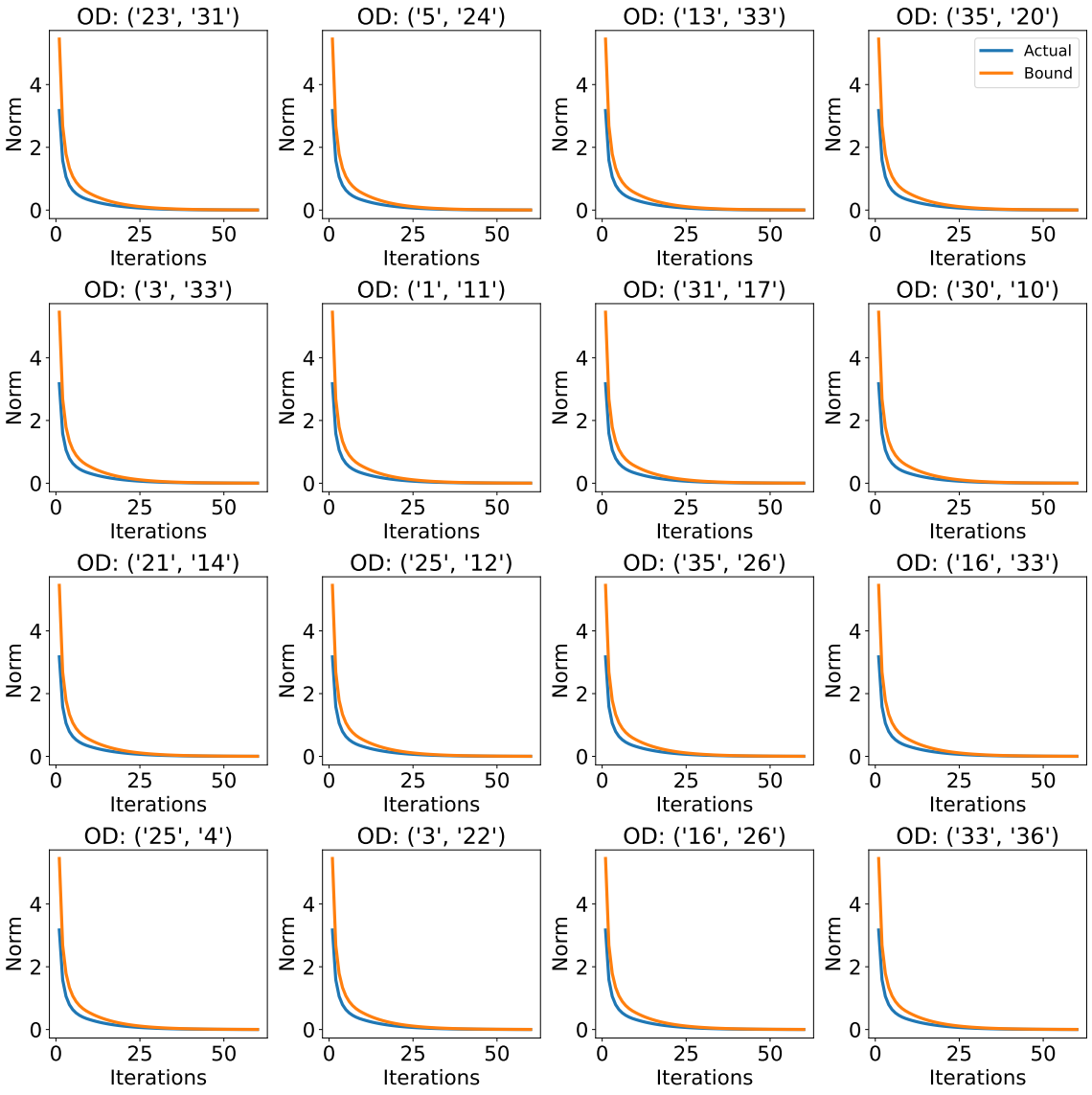

Figure 5.4: BMC - Path bound for 16 random OD pairs. The orange line represents the bound $M_{hr}^{OD}\|\mathcal{L}(\mathbf{h}) - \mathbf{h}\|_{OD}$, while the blue line depicts the actual distance from equilibrium $\|\hat{\mathbf{h}} - \mathbf{h}\|_{OD}$. The x-axis denotes the number of MSA iterations, and the y-axis represents the norm value.

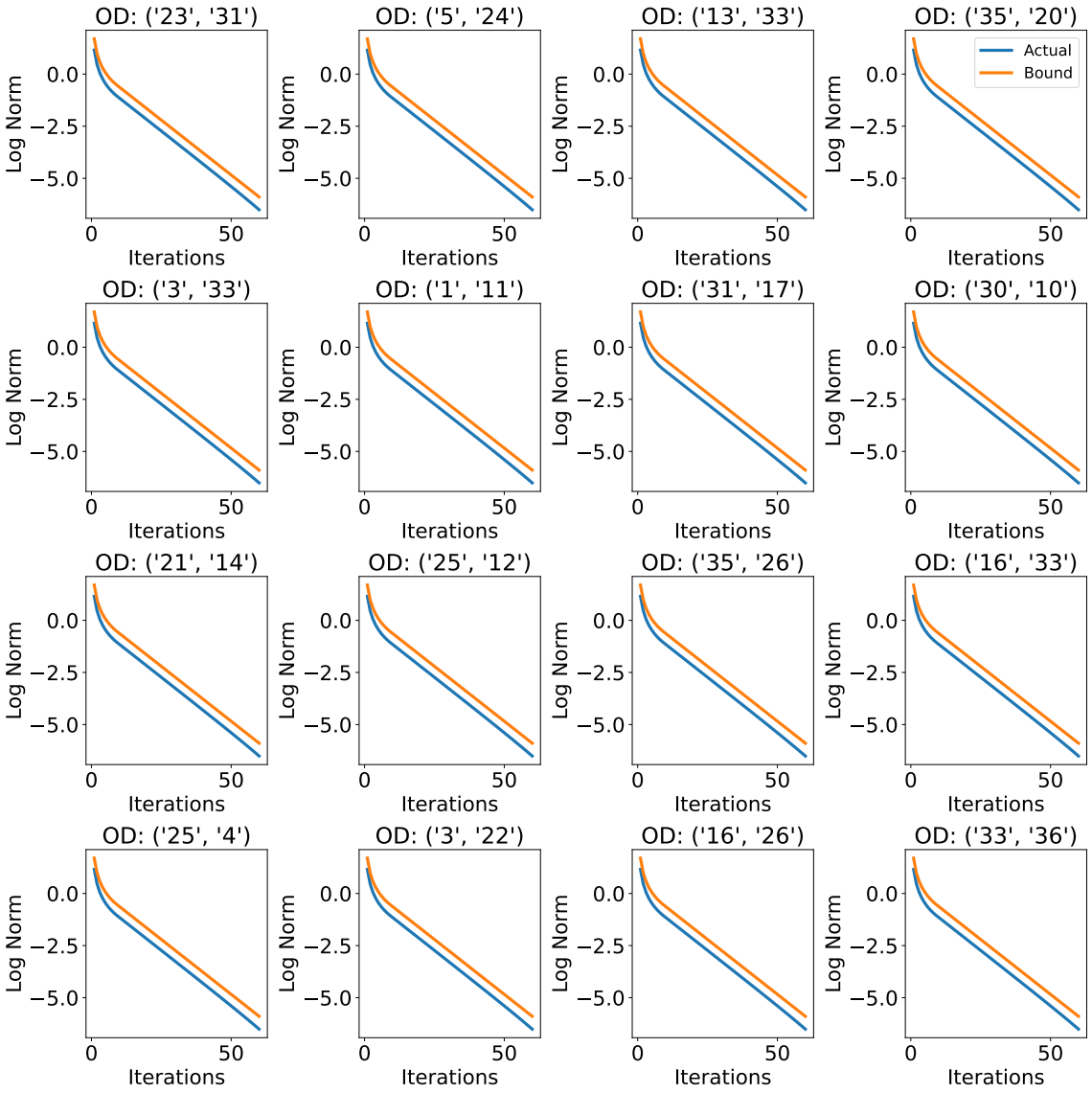

Figure 5.5: BMC - Semilog plot of all iterations for path bound for 16 random OD pairs. The orange line represents the bound $M_{hr}^{OD}\|\mathcal{L}(\mathbf{h}) - \mathbf{h}\|_{OD}$, while the blue line depicts the actual distance from equilibrium $\|\hat{\mathbf{h}} - \mathbf{h}\|_{OD}$. The x-axis denotes the number of MSA iterations, and the y-axis represents the log of the norm value.

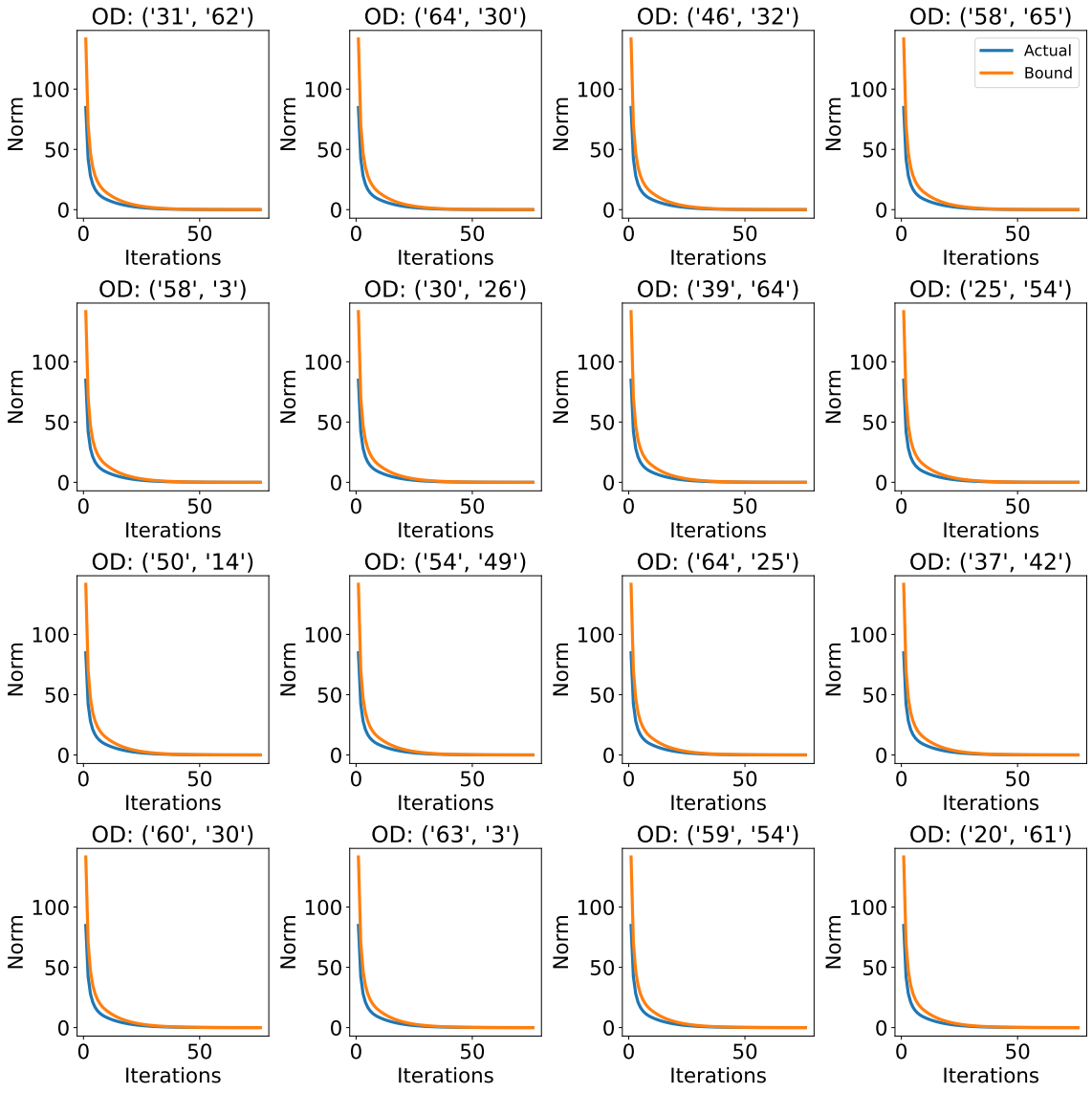

Figure 5.6: EMA - Path bound for 16 random OD pairs. The orange line represents the bound $M_{hr}^{OD}\|\mathcal{L}(\mathbf{h}) - \mathbf{h}\|_{OD}$, while the blue line depicts the actual distance from equilibrium $\|\hat{\mathbf{h}} - \mathbf{h}\|_{OD}$. The x-axis denotes the number of MSA iterations, and the y-axis represents the norm value.

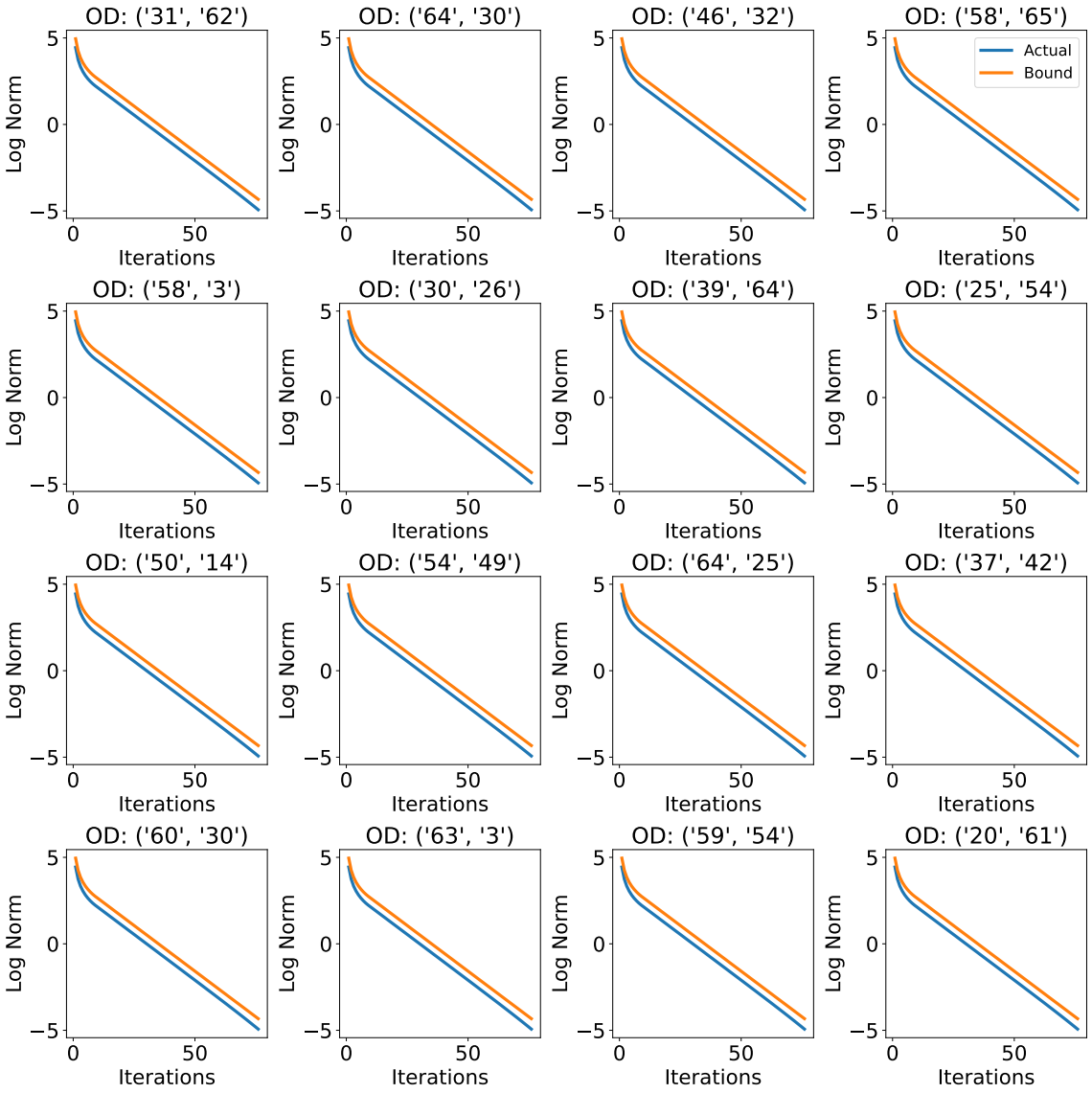

Figure 5.7: EMA - Semilog plot of all iterations for path bound for 16 random OD pairs. The orange line represents the bound $M_{hr}^{OD}\|\mathcal{L}(\mathbf{h}) - \mathbf{h}\|_{OD}$, while the blue line depicts the actual distance from equilibrium $\|\hat{\mathbf{h}} - \mathbf{h}\|_{OD}$. The x-axis denotes the number of MSA iterations, and the y-axis represents the log of the norm value.

Anaheim

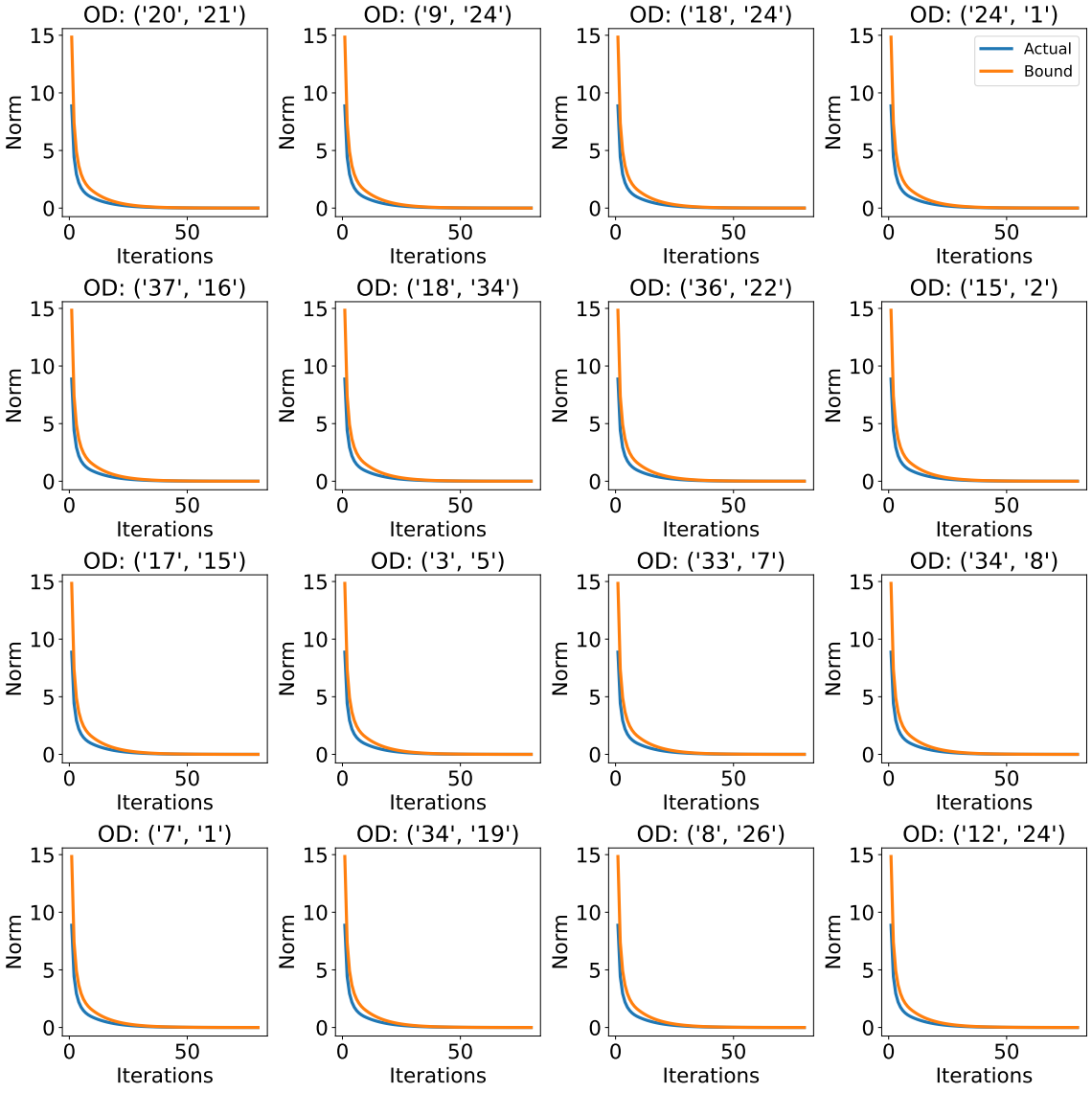

Figure 5.8: Anaheim - Path bound for 16 random OD pairs. The orange line represents the bound $M_{kr}^{OD}\|\mathcal{L}(\mathbf{h}) - \mathbf{h}\|_{OD}$, while the blue line depicts the actual distance from equilibrium $\|\hat{\mathbf{h}} - \mathbf{h}\|_{OD}$. The x-axis denotes the number of MSA iterations, and the y-axis represents the norm value.

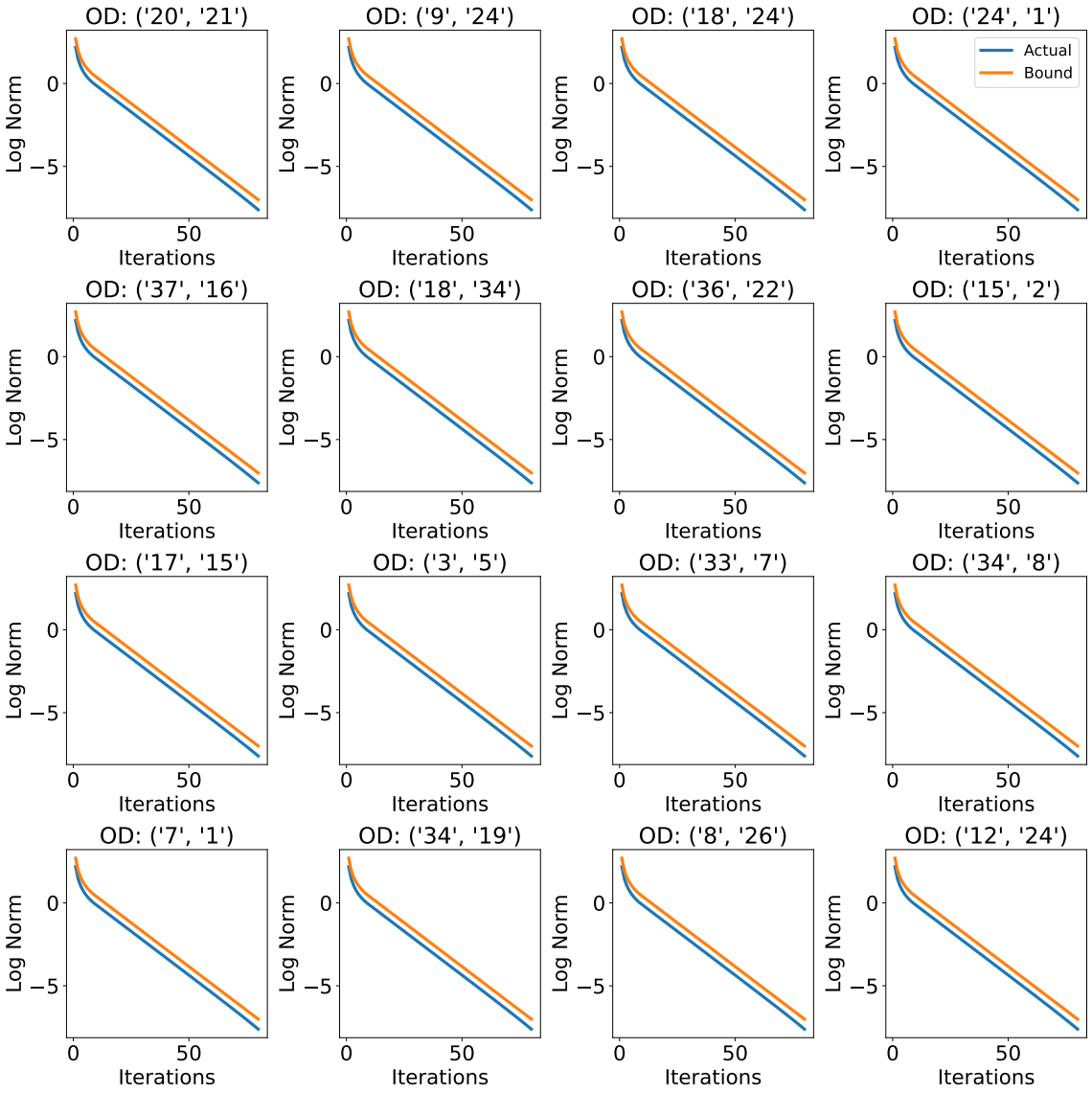

Figure 5.9: Anaheim - Semilog plot of all iterations for path bound for 16 random OD pairs. The orange line represents the bound $M_{hr}^{OD}\|\mathcal{L}(\mathbf{h}) - \mathbf{h}\|_{OD}$, while the blue line depicts the actual distance from equilibrium $\|\hat{\mathbf{h}} - \mathbf{h}\|_{OD}$. The x-axis denotes the number of MSA iterations, and the y-axis represents the log of the norm value.

To analyze the convergence of our bounds to equilibrium and assess the empirical convergence rate, we plot the bound gap (BG) between the derived upper bound and actual distance from equilibrium for each OD pair over consecutive iterations.

As expected, when the bound gap is plotted against iterations, we observe that the bound gap converges to zero in all OD pairs. The convergence plots for 16 random OD pairs in the Anaheim network are shown in Figure 5.10. Convergence plots for other networks are omitted for brevity; however, we present aggregate results on convergence on all four networks later.

To compute the convergence rate, we plot the ratio of the bound gap over consecutive iterations since we expect the bound gap to converge to zero. This plot eventually levels horizontally, indicating that the bound gap approaches zero at a linear rate close to equilibrium. We compute the convergence rate as the average of this ratio over the last 25 iterations. Figure 5.11 illustrates this technique for the Anaheim network. The mean and standard deviation (SD) of the convergence rate across all OD pairs are provided for each of the four networks in Table 5.5. Interestingly, it is observed that the convergence rate is similar across all the tested networks.

Network	**Convergence rate**	
	Mean	**SD**
Sioux Falls	0.91	0.03
BMC	0.91	0.00
EMA	0.91	0.00
Anaheim	0.91	0.00

Table 5.5: Convergence rate for different networks.

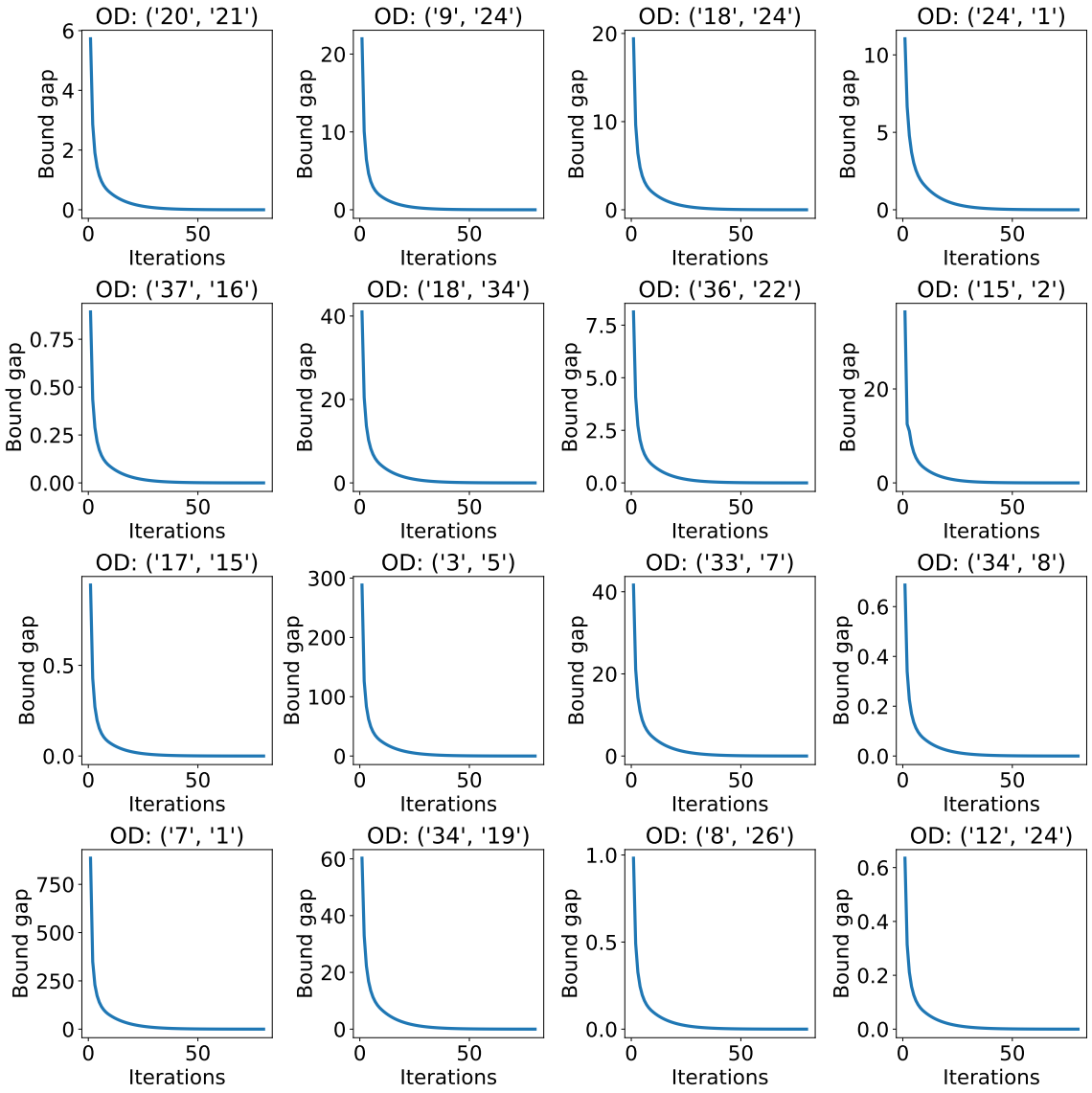

Figure 5.10: Anaheim - Convergence for 16 random OD pairs. The x-axis denotes the number of MSA iterations, and the y-axis represents the convergence value.

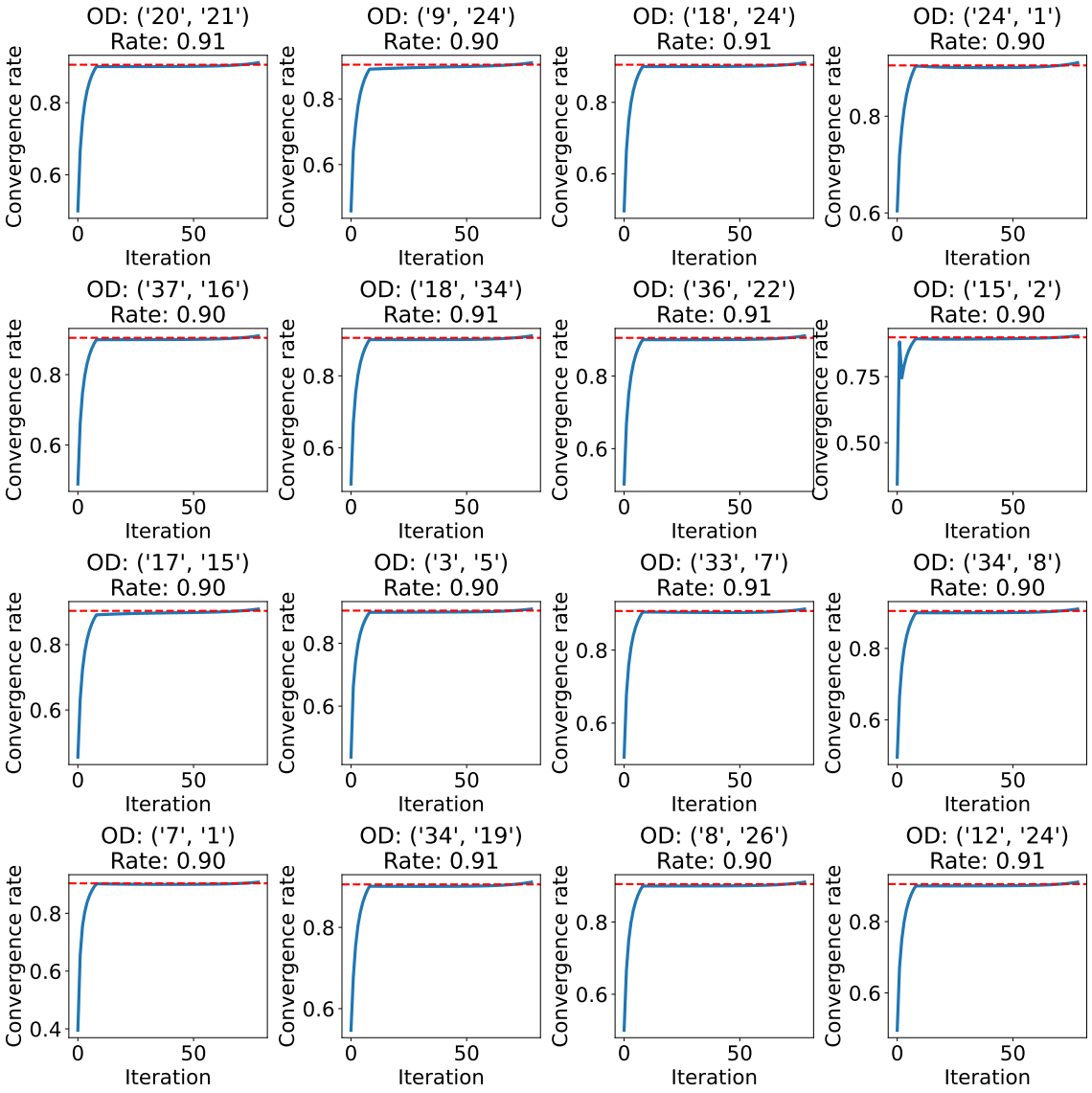

Figure 5.11: Anaheim - Rate of convergence for path bound for 16 random OD pair. The x-axis denotes the number of MSA iterations, and the y-axis represents the ratio of change in convergence over consecutive iterations.

5.2 Results on aggregate metrics

We present the results on the bounds for link flows, travel cost, and total system travel cost, as given in Lemmas 4 and 5. These results are summarized in figures in Tables 5.6, 5.7, and 5.8, respectively. The plots show the relative distance from equilibrium in blue, while the bound is represented in orange.

The figures illustrate the relative distance across all iterations and the last 20 iterations, as well as the absolute distance on a logarithmic scale for all iterations. The y-axis for both all iterations and the last 20 iterations represents the relative distance, defined as

$$\text{Relative distance} = \frac{\text{Distance from equilibrium (predicted or actual)}}{\text{Actual value at equilibrium}}. \tag{5.3}$$

These bounds are aggregated over all OD pairs in the network and are, therefore, not as tight as the path flow bounds. However, the results indicate they hold across all iterations. Moreover, the bounds on travel cost and link flows are reasonably tight near equilibrium. Further improvements are needed to improve the bounds on total system travel cost.

5.3 Application to bi-level traffic assignment

To demonstrate the applicability of our bounds in practice, we present a simple case study in network design. We solve the following problem: find the link in the network that, when closed, minimizes the absolute link cost norm. Such a problem is relevant if instances of Braes paradox-like scenarios have to be identified in a network. To simulate a closed link, we add a toll of \$100 (equivalent to a 25-minute delay) on that link. We test on the Sioux Falls network as it is the smallest network under study in this thesis and would allow us to fully enumerate the feasible sets to find the optimal solution.

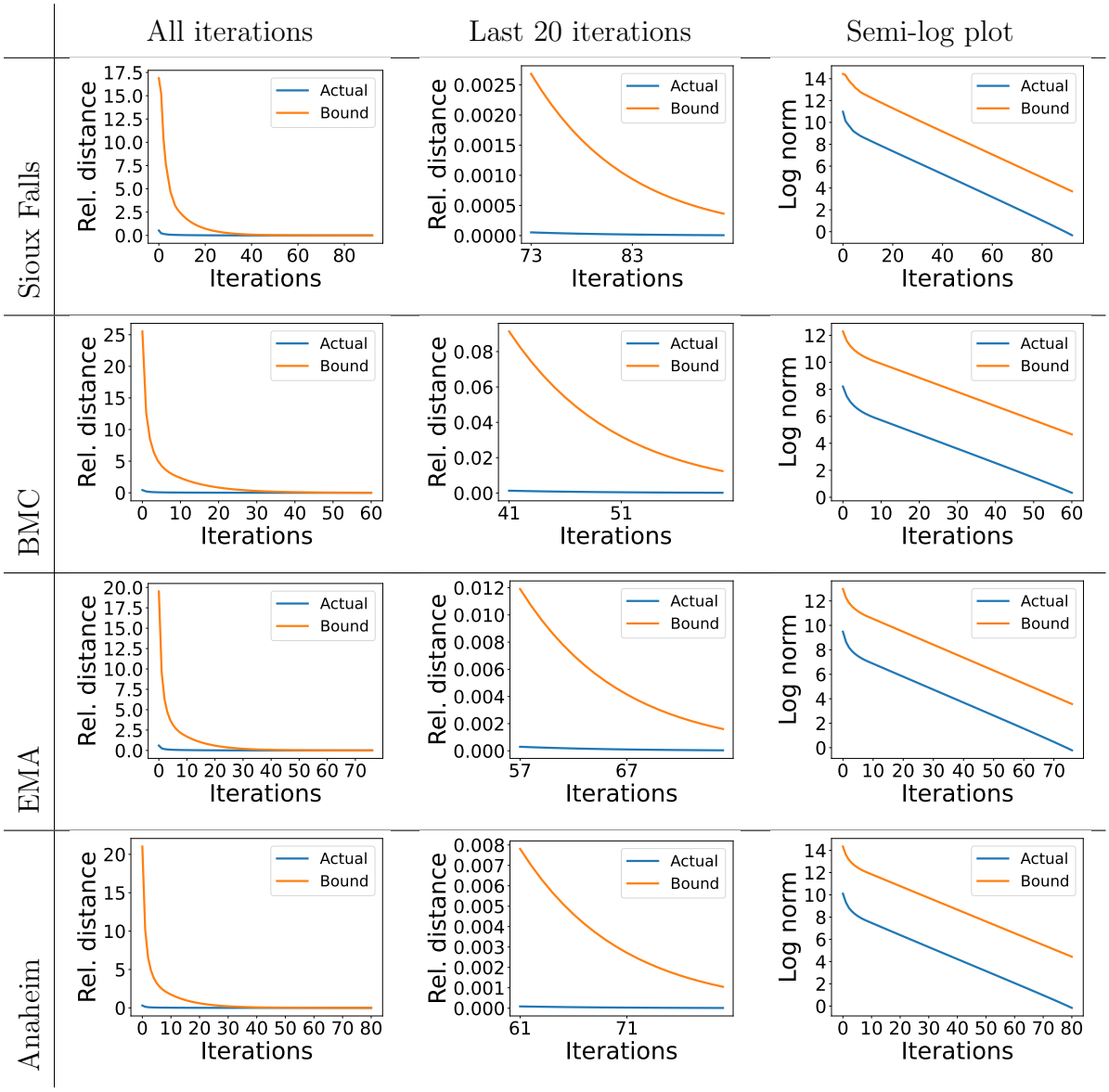

Table 5.6: Link flow bounds across networks — Relative (rel.) distance across iteration until a gap value of 10.

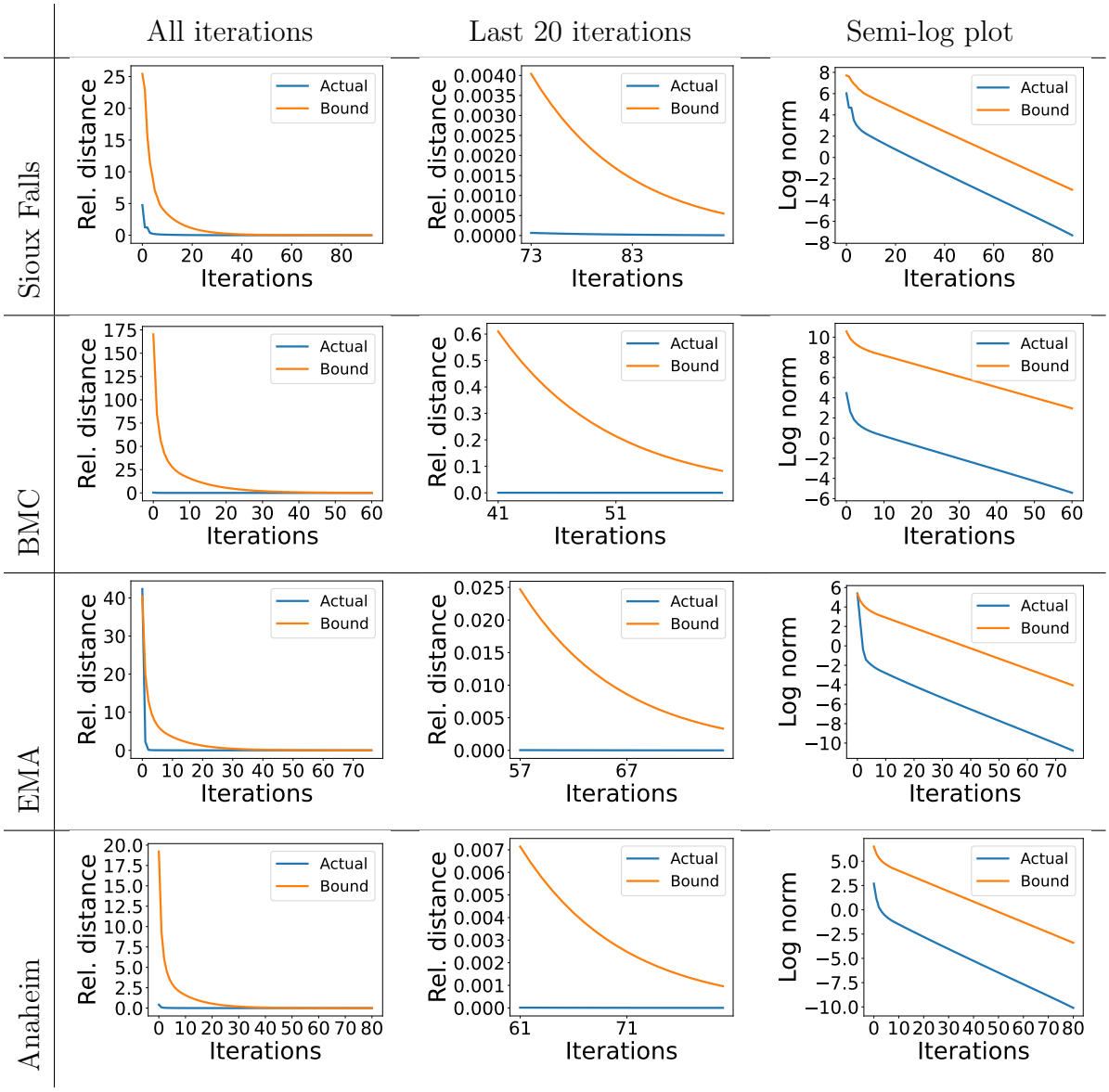

Table 5.7: Travel time bounds across networks — Relative (rel.) distance across iteration until a gap value of 10.

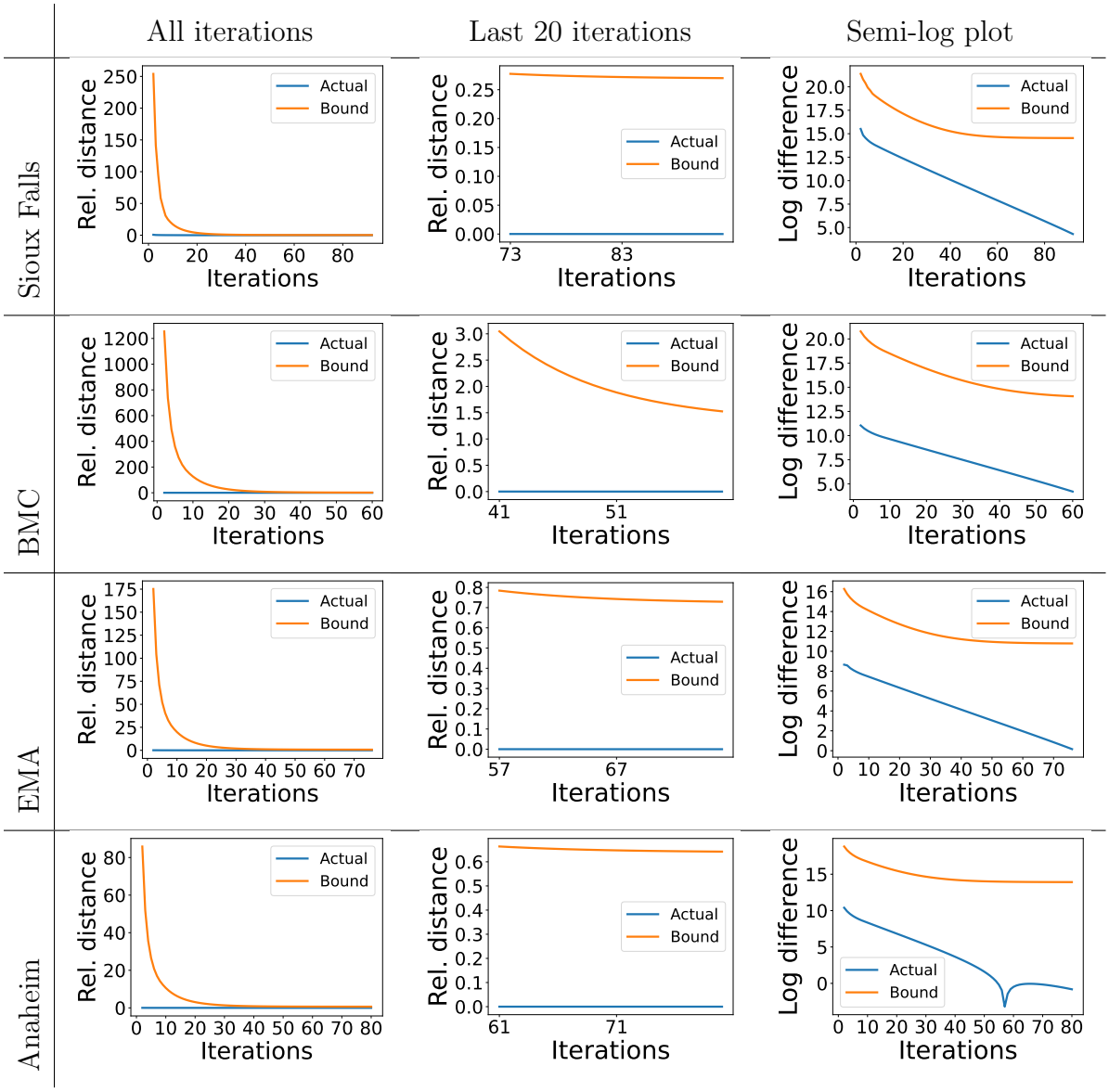

Table 5.8: TSTT bounds across networks — relative (rel.) distance across iteration until a gap value of 10.

We first solve the problem by exhaustively enumerating the feasible set. Each link of the network is closed individually, and a traffic assignment run is performed. The resultant norm of link cost is then checked. This way, the link that, when closed, would produce the least link cost norm could be obtained. All the traffic assignment problems are solved to optimality (i.e., until $\|\mathbf{h} - \mathcal{L}(\mathbf{h})\| \leq 1$). Algorithm 3 summarizes this procedure.

Algorithm 3 Simple network design without using bounds

for $l \in \mathbb{L}$ **do**

(a.) Apply a high toll on link l to simulate its closure.
(b.) Run traffic assignment until **gap = 1**
(c.) Compute the norm of link flows.
(d.) Record the closed link and the corresponding link cost norm.

To solve the same problem using the bounds derived in Chapter 4, we first decide the available computation budget and the gap value until we solve each traffic assignment run. Using this gap value, we select the smallest corresponding r value, ensuring the bounds remain valid. For our experiment on the Sioux Falls network, we set the stopping gap value of 100. Referring to Table 5.4, we identify that the smallest r value for the bound to be applicable beyond this gap is 0.3.

Following the same complete enumeration approach, we solve the traffic assignment problems but only until the stopping gap value of 100. At the final iteration, we record the link cost norm and the upper bound value. We estimate the range of the equilibrium link cost norm by adding or subtracting the cost norm and the upper bound on its distance from equilibrium. Using this estimate, we identify the optimal link to be closed. The entire procedure is outlined in Algorithm 4.

Algorithm 4 Simple network design using bounds

for $l \in \mathbb{L}$ **do**

(a.) Apply a high toll on link l to simulate its closure.
(b.) Run traffic assignment until **gap = 1000**
(c.) Compute both the norm of link flows and an upper bound on the distance between the current and equilibrium link flows.
(d.) Estimate equilibrium link flow norm = norm of the current link flows ± upper bound on the distance between the current and equilibrium link flows.
(e.) Record the closed link and the corresponding estimated maximum equilibrium link cost norm.

Table 5.9 presents the results of the top 5 links and corresponding link cost norm obtained using both procedures. Both methods returned the same top five links to be closed with the least link cost norm. However, the same result was obtained 36.2% faster using bounds (16.7 minutes using bounds compared to 26.2 minutes without). As the network size grows, we expect an even more striking improvement in run time by using the bounds.

Without using bounds			With using bounds				
Rank	Link	Cost norm	Rank	Link	Cost norm (current)	Upper bound	Estimated cost norm (equilibrium)
1	(24, 23)	**92.59**	1	(24, 23)	92.60	0.40	[92.20, **93.01**]
2	(23, 24)	**92.62**	2	(23, 24)	92.62	0.42	[92.20, **93.05**]
3	(19, 17)	**92.89**	3	(19, 17)	92.89	0.38	[92.51, **93.29**]
4	(17, 19)	**93.05**	4	(17, 19)	93.05	0.39	[92.66, **93.44**]
5	(12, 13)	**93.60**	5	(12, 13)	93.61	0.39	[93.22, **94.00**]
Total time taken: 26.2 min			Total time taken: 16.7 min				

Table 5.9: Comparison of link cost norms with and without using bounds. The links and the corresponding equilibrium link cost norm (shown boldfaced) are the outputs of each algorithm.

Chapter 6: Discussions and conclusion

6.1 Summary

In this thesis, we derive local upper bounds on the distance of path flows, link flows, travel costs, and total system travel costs from the corresponding equilibrium solution. These bounds are local and, hence, only apply near the equilibrium solution. A detailed analysis of the tightness and the distance from equilibrium at which these bounds become applicable is also provided. We show the bounds on the distance of path flows, link flows, and link costs are tight in a network of parallel links with constant and equal link costs. Further, empirical results on the rate of convergence indicate a nearly linear rate of convergence close to equilibrium.

We find that the path flow bounds can be computed quickly and efficiently, and they remain applicable even at a relatively large distance from equilibrium while staying sufficiently tight across all four tested networks. The link flow and travel cost bounds apply to all iterations of MSA and are found to be reasonably tight. However, the bounds on total system travel cost are extremely loose.

We now discuss how our results can be applied in practice. When used as a stopping criterion in a traffic assignment subproblem while evaluating multiple alternatives, these upper bounds can provide valuable insights into the behavior of the equilibrium solution for each subproblem, allowing early termination for poor alternatives. Decision-makers can use these bounds to determine an appropriate stopping criterion based on aggregate metrics of interest. We present a small network design example to identify optimal link closures and demonstrate the practical applicability of the bounds. We perform a complete enumeration of the feasible set to determine the optimal link for closure. On the Sioux Falls network, the use of the derived bounds yields a 36% reduction in computation time relative to the case without bounds.

Further, the derived bounds provide a theoretical background on the empirical results on gap measures and convergence of traffic assignment problems proposed in Boyce et al. (2004) and Patil et al. (2021). Even when the bounds derived in this thesis are not used as a stopping criterion, they can offer insight into the possible range of equilibrium values for any feasible solution close to equilibrium.

6.2 Limitations and future work

We acknowledge several limitations of this study. Without a global bound, it is impossible to determine the distance from equilibrium beyond which the local bound becomes applicable. Extending local bounds to global ones is challenging, as the parameter r in Theorem 8 cannot be arbitrarily large. While our empirical studies provide estimates for when these bounds become reliable, a global bound would offer greater confidence in their applicability.

Furthermore, the computational effort spent in calculating these bounds should be improved. If the computation is too costly, it defeats the purpose of applying the bounds as opposed to performing additional iterations to improve path flows. For instance, in the Sioux Falls network, the computation of bounds took around 0.07s, while each iteration of the MSA took around 0.18s. However, state-of-the-art traffic assignment solvers can solve each iteration significantly faster. A significant future direction in improving the derived bounds would be to find ways to reduce the computational effort in computing them. Matrix algebra techniques in norm estimation are one such way this can be achieved. These could include ways of using a less computationally expensive norm, such as the Frobenius norm, or using an approximation of the norm.

Finally, the bounds derived for total system travel costs are found to be very loose. Our approach relies only on bounds for link flows and travel costs to estimate total system travel cost bounds. However, incorporating additional information on the demand for each OD pair could significantly improve these estimates (as these

bound the feasible region much better than just the bounds on link flows and travel costs). The SUE also satisfies a path variational inequality (VI) formulation. Such formulations are often used to bound the price of anarchy in SUE (Guo et al., 2010). The VI formulation, along with bounds on path flows and path costs, can be used to derive a bound on total system travel cost. While these extensions are nontrivial, they present a promising direction for future research.

Works Cited

Tom M Apostol and CM Ablow. Mathematical analysis, 1958.

Hillel Bar-Gera. Origin-based algorithm for the traffic assignment problem. *Transportation Science*, 36(4):398–417, 2002.

Hillel Bar-Gera. Traffic assignment by paired alternative segments. *Transportation Research Part B: Methodological*, 44(8-9):1022–1046, 2010.

Hillel Bar-Gera and David Boyce. Solving a non-convex combined travel forecasting model by the method of successive averages with constant step sizes. *Transportation Research Part B*, 40:351–367, 2006.

Sharminda Bera and KV Rao. Estimation of origin-destination matrix from traffic counts: the state of the art. 2011.

David Boyce, Biljana Ralevic-Dekic, and Hillel Bar-Gera. Convergence of traffic assignments: how much is enough? *Journal of Transportation Engineering*, 130 (1):49–55, 2004.

Stephen D Boyles and Natalia Ruiz Juri. Queue spillback and demand uncertainty in dynamic network loading. *Transportation Research Record*, 2673(2): 38–48, 2019.

Stephen D Boyles, Nicholas E Lownes, and Avinash Unnikrishnan. Transportation network analysis. *Vol. I: Static and Dynamic Traffic Assignment*, 2020.

Stephen D. Boyles, Nicholas E. Lownes, and Avinash Unnikrishnan. *Transportation Network Analysis*, volume 1. 2025. edition 1.0.

Bureau of Public Roads. *Traffic assignment manual for application with a large, high speed computer*, volume 37. US Department of Commerce, Bureau of Public Roads, Office of Planning, Urban Planning Division, 1964.

Giulio Erberto Cantarella and Ennio Cascetta. Stochastic assignment to transportation networks: models and algorithms. In *Equilibrium and advanced transportation modelling*, pages 87–107. Springer, 1998.

Richard Courant, Fritz John, Albert A Blank, and Alan Solomon. *Introduction to calculus and analysis*, volume 1. Springer, 1965.

Abigail J. Crocker. *Postdisaster Transportation Network Recovery*. Doctoral dissertation, University of Texas at Austin, 2024.

Carlos F Daganzo and Yosef Sheffi. On stochastic models of traffic assignment. *Transportation science*, 11(3):253–274, 1977.

André De Palma and Robin Lindsey. Traffic congestion pricing methodologies and technologies. *Transportation Research Part C: Emerging Technologies*, 19 (6):1377–1399, 2011.

Robert B Dial. A probabilistic multipath traffic assignment model which obviates path enumeration. *Transportation research*, 5(2):83–111, 1971.

Robert B Dial. A path-based user-equilibrium traffic assignment algorithm that obviates path storage and enumeration. *Transportation Research Part B: Methodological*, 40(10):917–936, 2006.

Said M Easa. Traffic assignment in practice: overview and guidelines for users. *Journal of Transportation Engineering*, 117(6):602–623, 1991.

Francisco Facchinei and Jong-Shi Pang. *Finite-dimensional variational inequalities and complementarity problems*. Springer, 2003.

Caroline Fisk. Some developments in equilibrium traffic assignment. *Transportation Research Part B: Methodological*, 14(3):243–255, 1980.

Gerald B Folland. Higher-order derivatives and taylor's formula in several variables. *Preprint*, 1, 2005. http://sites.math.washington.edu/~folland/Math425/taylor2.pdf.

Nicola Fusco, Paolo Marcellini, and Carlo Sbordone. *Mathematical Analysis*. Springer, 2023.

Theodore Gamelin. *Complex analysis*. Springer Science & Business Media, 2003.

Guido Gentile. Local user cost equilibrium: a bush-based algorithm for traffic assignment. *Transportmetrica A: Transport Science*, 10(1):15–54, 2014.

James E Gentle. Matrix algebra. *Springer texts in statistics, Springer, New York, NY, doi*, 10:978–0, 2007.

Can Gokalp, Priyadarshan N Patil, and Stephen D Boyles. Post-disaster recovery sequencing strategy for road networks. *Transportation research part B: methodological*, 153:228–245, 2021.

Xiaolei Guo and Da Xu. Profit maximization by a private toll road with cars and trucks. *Transportation Research Part B: Methodological*, 91:113–129, 2016.

Xiaolei Guo, Hai Yang, and Tian-Liang Liu. Bounding the inefficiency of logit-based stochastic user equilibrium. *European Journal of Operational Research*, 201(2):463–469, 2010.

Highway Capacity Manual. Highway capacity manual. *Washington, DC*, 2(1): 1, 2000.

Takamasa Iryo. Properties of dynamic user equilibrium solution: existence, uniqueness, stability, and robust solution methodology. *Transportmetrica B: Transport Dynamics*, 1(1):52–67, 2013.

Yu Jiang. A variational inequality formulation for stochastic user equilibrium with a bounded choice set. *Computers & Operations Research*, 167:106677, 2024.

Frank H Knight. Some fallacies in the interpretation of social cost. *The Quarterly Journal of Economics*, 38(4):582–606, 1924.

Frank S Koppelman and Chandra Bhat. A self instructing course in mode choice modeling: multinomial and nested logit models. 2006.

Yannis A Korilis, Aurel A Lazar, and Ariel Orda. Avoiding the braess paradox in non-cooperative networks. *Journal of Applied Probability*, 36(1):211–222, 1999.

Daniel A Lazar, Samuel Coogan, and Ramtin Pedarsani. The price of anarchy for transportation networks with mixed autonomy. In *2018 Annual American Control Conference (ACC)*, pages 6359–6365. IEEE, 2018.

Hao Li, Michiel CJ Bliemer, and Piet HL Bovy. Network reliability-based optimal toll design. *Journal of Advanced Transportation*, 42(3):311–332, 2008.

Hans Lindblad. Lecture 9: 4.1 taylor's formula in several variables, sep 2011. URL https://math.jhu.edu/~lindblad/211/l9.pdf. Accessed: 2025-02-23.

Robin Lindsey* and Erik Verhoef*. Traffic congestion and congestion pricing. In *Handbook of transport systems and traffic control*, pages 77–105. Emerald Group Publishing Limited, 2001.

Wenteng Ma, Ruey Long Cheu, and Der-Horng Lee. Scheduling of lane closures using genetic algorithms with traffic assignments and distributed simulations. *Journal of Transportation Engineering*, 130(3):322–329, 2004.

Mike Maher. Algorithms for logit-based stochastic user equilibrium assignment. *Transportation Research Part B: Methodological*, 32(8):539–549, 1998.

Richard Mounce and Malachy Carey. On the convergence of the method of successive averages for calculating equilibrium in traffic networks. *Transportation science*, 49(3):535–542, 2015.

Yu Nie. A note on bar-gera's algorithm for the origin-based traffic assignment problem. *Transportation Science*, 46(1):27–38, 2012.

Priyadarshan N Patil, Katherine C Ross, and Stephen D Boyles. Convergence behavior for traffic assignment characterization metrics. *Transportmetrica A: Transport Science*, 17(4):1244–1271, 2021.

Neil J Pedersen and Donald R Samdahl. Highway traffic data for urbanized area project planning and design. *NCHRP Report*, (255), 1982.

Arthur Cecil Pigou. *The Economics of Welfare*. Macmillan, 1924.

Joseph N Prashker and Shlomo Bekhor. Route choice models used in the stochastic user equilibrium problem: a review. *Transport reviews*, 24(4):437–463, 2004.

Charles Chapman Pugh and CC Pugh. *Real mathematical analysis*, volume 2011. Springer, 2002.

David Rey and Hillel Bar-Gera. Long-term scheduling for road network disaster recovery. *International journal of disaster risk reduction*, 42:101353, 2020.

Diego Martin Robalino Muñoz. *Equitable tolling: a case study on Sioux Falls*. PhD thesis, 2024.

Geoffrey Rose, Mark S Daskin, and Frank S Koppelman. An examination of convergence error in equilibrium traffic assignment models. *Transportation Research Part B: Methodological*, 22(4):261–274, 1988.

Tim Roughgarden. The price of anarchy is independent of the network topology. In *Proceedings of the thiry-fourth annual ACM symposium on Theory of computing*, pages 428–437, 2002.

Tim Roughgarden. *Selfish routing and the price of anarchy*. MIT press, 2005.

Arne Schneck and Klaus Nökel. Accelerating traffic assignment with customizable contraction hierarchies. *Transportation research record*, 2674(1):188–196, 2020.

Bing-Feng Si, Ming Zhong, Hao-Zhi Zhang, and Wen-Long Jin. An improved dial's algorithm for logit-based traffic assignment within a directed acyclic network. *Transportation planning and technology*, 33(2):123–137, 2010.

Transportation Networks for Research Core Team. Transportation networks for research, 2025. https://github.com/bstabler/TransportationNetworks. Accessed 2025-02-28.

William S Vickrey. Pricing in urban and suburban transport. *The American Economic Review*, 53(2):452–465, 1963.

William S Vickrey. Congestion theory and transport investment. *The American economic review*, 59(2):251–260, 1969.

Luis G Willumsen. Estimation of an od matrix from traffic counts–a review. 1978.

Hai Yang. Heuristic algorithms for the bilevel origin-destination matrix estimation problem. *Transportation Research Part B: Methodological*, 29(4):231–242, 1995.

Hai Yang and Michael G. H. Bell. Models and algorithms for road network design: a review and some new developments. *Transport Reviews*, 18(3):257–278, 1998a.

Hai Yang and Michael GH Bell. A capacity paradox in network design and how to avoid it. *Transportation Research Part A: Policy and Practice*, 32(7):539–545, 1998b.

Jing Zhang, Sepideh Pourazarm, Christos G Cassandras, and Ioannis Ch Paschalidis. The price of anarchy in transportation networks: Data-driven evaluation and reduction strategies. *Proceedings of the IEEE*, 106(4):538–553, 2018.

Zirui Zhou and Anthony Man-Cho So. A unified approach to error bounds for structured convex optimization problems. *Mathematical Programming*, 165: 689–728, 2017.

Vita

Debojjal Bagchi is originally from Kolkata, India. In 2023, he graduated with a Bachelor of Science (Research) from the Indian Institute of Science, Bangalore, earning first-class distinction. He then joined the graduate program in the Cockrell School of Engineering's Department at Civil, Architectural, and Environmental Engineering at the University of Texas at Austin, where he became a member of Dr. Boyle's Simulation, Pricing, Adaptive Routing, and Traffic Assignment (SPARTA) lab. Debojjal's research interests include traffic assignment, multi-modal networks, and network optimization.

Address: debojjalb@utexas.edu

This thesis was typeset with LaTeX[†] by the author.

[†]LaTeX is a document preparation system developed by Leslie Lamport as a special version of Donald Knuth's TeX Program.